UNIVERSITAT POLITÈCNICA DE CATALUNYA
BARCELONATECH

Escola Superior d'Enginyeries Industrial, Aeroespacial i Audiovisual de Terrassa

MASTER'S DEGREE IN SPACE AND AERONAUTICAL ENGINEERING

Development of Computational Fluid dynamic codes for the numerical resolution of the Navier-Stokes equations applied to benchmark problems using finite volume method.

Author

Boris Marcial Ortega Varas

Director

Asencio Oliva Llena

Co-Director

Carlos David Perez Segarra

Fall 2018

I declare that,

The work in this Master Thesis is completely my own work,

No part of this Master Thesis is taken from other people's work without giving them credit,

all references have been clearly cited,

I understand that an infringement of this declaration leaves me subject to the foreseen disciplinary actions by *The Universitat Politècnica de Catalunya - BarcelonaTECH*.

Boris Marcial Ortega Varas Fall 2018

Development of Computational Fluid dynamic codes for the numerical resolution of the Navier-Stokes equations applied to benchmark problems using finite volume method.

Acknowledgment

Prima di tutto vorrei iniziare ringraziando una persona molto speciale Ines Capellaro, sei stata una persona di un cuore grande e se ora sono qui e' anche merito tuo, non sei piu' con noi ma la tua memoria rimarra' sempre nel mio cuore.

Ringrazio i miei genitori per avermi sostenuto sempre anche nei momenti difficili, siete stati una parte fondamentale del mio percorso Accademico. Mia nonna Cruz che ha sempre creduto in me e mi ha spronato ad andare avanti.

Ringrazio la Universita' Politecnica di Catalunya per avermi dato la possibilita' di fare parte di questa rinomata istituzione. Ringrazio i professori Carlos David Perez Segarra e Asensio Oliva per i loro consigli e l'appoggio datomi durante la realizzazione di questo progetto.

Per ultimo vorrei ringraziare a tutte quelle persona che mi sono state vicine durante il mio percorso accademico .

First of all, I would like to start by thanking a very special person, Ines Capellaro, you have been a person with a big heart and if I am here now it is also your merit, you are no longer with us but your memory will always remain in my heart.

I thank my parents for always supporting me even in difficult moments, you have been a fundamental part of my academic career. My grandmother Cruz who always believed in me and encouraged me to keep going.

I thank the Polytechnic University of Catalonia for giving me the chance to be part of this renowned institution. I thank the professors Carlos David Perez Segarra and Asensio Oliva for their advices and support given to me during the realization of this project.

Finally, I would like to thank all those who have been close to me during my academic career.

ABSTRACT

The main objective of this work is the development of different programs to learn and verify computational fluid dynamics problems which are governed by the Navier-Stokes equations.

The document will be divided into different chapters in which we will detail the procedures performed.

During the first chapter there will be an introduction on computational fluid dynamics problems, as the basic requirements to deal with this type of cases, as well as the limits that will be encountered during the development of these.

In the second chapter there will be a brief introduction about the necessary theory which will be of great help during the development of the case studies.

The convection-diffusion equations will be studied in the third chapter, which will be discretized for the development of the different cases. In this chapter we will also introduce the concept of Finite volume method that will be a fundamental part of this work. Finally, we will see the different numerical schemes that can be implemented, as well as the different solvers.

During the fourth chapter the different cases will be presented, such as the Transient Conduction problem, the Diagonal flow and the Smith Hutton problem, which will be developed and commented.

In the fifth chapter we will introduce in the Fractional Step Method, we will see the different steps to follow for the implementation of this method in the development of the case the Driven Cavity. the spatial discretization and the algorithm necessary for the development of this will be detailed. Finally, the results will be discussed, and the pertinent conclusions will be given.

We will make an introduction to the field of turbulence that is why in chapter six the Burgers equations will be discretized; two different methods will be studied LES (Large eddy simulation) and DNS (Direct numerical simulation). The results obtained will be compared with the references given by the CTTC.

RESUMEN

El objetivo principal de este trabajo es el desarrollo de diferentes programas para aprender y verificar problemas de fluidodinámica computacional las cuales son gobernadas por las ecuaciones de Navier-Stokes.

El documento será dividido en diferentes capítulos en los cuales detallaremos los procedimientos realizados.

Durante el primer capítulo se hará una introducción sobre los problemas de fluidodinámica computacional, como los requisitos bases para afrontar este tipo de casos, así como los límites que se encontraran durante el desarrollo de estos.

En el segundo capítulo se hará una breve introducción sobre la teoría necesaria la cual será de gran ayuda durante el desarrollo de los casos de estudio.

Las ecuaciones de convection-diffusion se estudiarán en el tercer capítulo las cuales serán discretizadas para el desarrollo de los diferentes casos. En este capítulo también se introducirá al concepto de Finite volume method que será parte fundamental de este trabajo. Por último, veremos los diferentes esquemas numéricos que se pueden implementar, así como los diferentes solvers.

Durante el cuarto capítulo se presentarán los diferentes casos como the Transient Conduction problem, Diagonal flow y Smith Hutton problem los cuales serán desarrollados y comentados durante este capítulo.

En el quinto capítulo nos introduciremos en el Fractional Step Method, veremos los diferentes pasos a seguir para la implementación de este método en el desarrollo del caso the Driven Cavity. se detallará la discretización espacial y el algoritmo necesario para el desarrollo de este. por último, se comentarán los resultados y se darán las conclusiones pertinentes.

Haremos una introducción en el campo de la turbulencia por eso en el capítulo seis se discretizarán las ecuaciones de Burgers, se estudiarán dos diferentes métodos LES (Large eddy simulation) y DNS (Direct Numerical Simulation). Los resultados obtenidos serán confrontados con las referencias dadas por la CTTC.

CONTENTS

LIST OF FIGURES

LIST OF TABLES

1.Introduction

1.1 Aim of the study

The fundamental purpose of this project consists of the creation of a code programmed with MatLab that allows solving the Navier-Stokes equations in their incompressible form and studying the phenomenology of fluid mechanics and the bases of computational fluid dynamics. The main idea is to deepen the physics behind the process of computational implementation of a problem, so the code will solve cases with simple geometries. Spatial discretization has been proposed using the finite volume method and the fractional steps method has been used to solve the velocity and pressure coupling for the Driven Cavity case and the discretization of the convection-diffusion equations for the other cases. Large Eddy Simulation (LES) and Direct Numerical Simulation (DNS) to solve the burgers equation.

1.2 Requirements

The necessary requirement for the realization of these cases is the knowledge of a programming language MATLAB will use for this project. Another type of requirement is to use a type of mesh that approaches the reality of the problem to achieve values more similar to the references.

1.3 Justification

The advantages presented by the simulation against other analysis tools will be commented and, in this way, understand the reasons for which computer simulation has been chosen as the basis of this project. Today, simulation is both an alternative and a complement to experimentation in many branches of science since it is a cheap and effective tool for predicting the properties and behavior of a physical system. Not only that, but the computational techniques are a necessary complement to the theory that allows to verify the consequences that are obtained from performing hypotheses or complex models in different branches of physics, and that otherwise cannot be checked.

The simulations allow us to systematically improve the design and properties of materials through the optimization of algorithms. A procedure without simulations will be tremendously expensive if it is done by prototyping or by other means of experimentation. Then it can be said that simulation is a tool that improves the efficiency of technological processes.

In the simulations, specifically in the field of computational fluid dynamics because the prediction of cases is so complicated that it cannot be resolved analytically, it is where the simulation contributes more benefits and its use is more than justified.

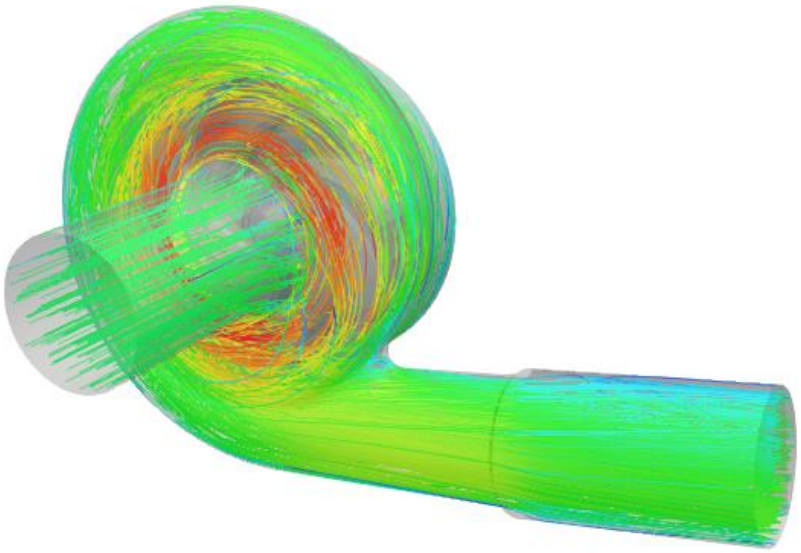

Figure 1: Example of a Centrifugal Pump in CFD simulation.

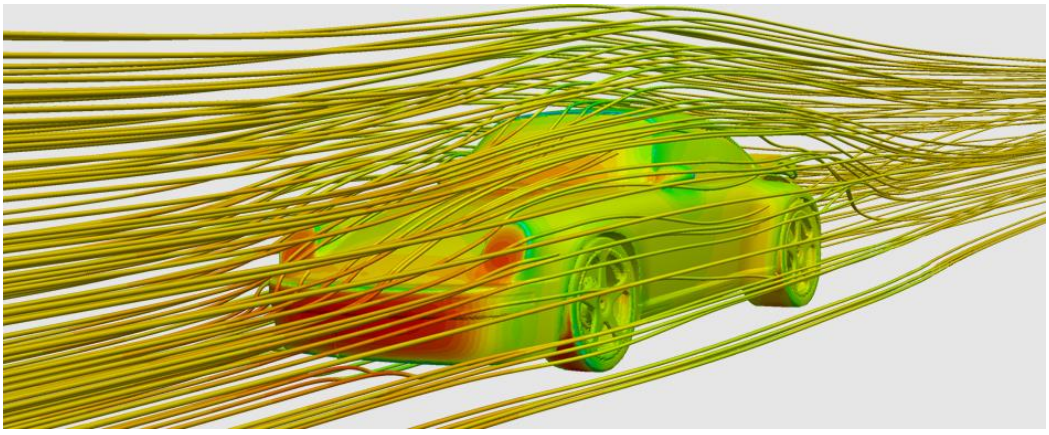

Figure 2: Example of a flow across a car CFD simulations.

As already mentioned, this project aims to deepen the physical phenomenology of fluid mechanics, as well as the computational foundations of simulation with CFD tools to achieve a solid base in this field of physics.

Therefore, we must understand the philosophy of this project to understand the operation of the very complex computational tools that exist today. For this reason, it has been decided to create an own code instead of using tools already in use such as ANSYS Fluent, OpenFoam or RealFlow among others. Although these programs are very useful for fluid simulation, their high complexity makes them not the most adequate tools to understand in detail how the equations of fluid mechanics are solved.

1.4 Limitation

Before introducing the theoretical contents related to the project, it is necessary to specify certain points that affect its scope:

- Since the phenomena treated in fluid dynamics are macroscopic, we will assume the hypothesis of mass continuity. This implies that any volume element will be sufficiently large to contain a very large number of molecules.
- The physical properties of the fluid will always be considered constant within the range of application of the equations. This implies that you work with incompressible fluids.
- The work regime will be laminar, so it will not be possible to solve cases with flows in a turbulent state.
- The program will work with two-dimensional problems.

2.Matematical Formulation

2.1 Introduction

In this chapter we will briefly review the theory needed to tackle this project. It begins with the classification of fluids that will help us later when considering the resolution of problems, that is, during this project we will assume some necessary hypotheses to study the Navier-Stokes equations. We will see the conservation of the mass and momentum; these definitions of conservation will be great help and simplify the numerical resolution that we will see throughout this work.

Another fundamental parameter of this project is the Reynolds number, we will make a brief introduction and analyze how this parameter contributes when solving the Navier-Stokes equations. Finally, the contour equations will be studied which will be applied to the different cases of studies that we will face in this work.

2.2 Fluids classification

- Steady – Non-steady

A steady flow is one in which the variables that define it do not change locally over time. A transient one in which they do.

- Incompressible – Compressible

An incompressible fluid is one in which we can consider its density as constant; otherwise, the fluid is called compressible.

- Ideal – Viscous

An ideal fluid is one in which the effect of viscosity is so weak that it can be assumed to be zero. This means that we can neglect the internal friction force between the different layers of fluid. On the other hand, the fluids in which the dominant effect is viscosity, are called viscous.

- Newtonian

Newtonian fluids are those in which the viscosity is constant, it means, the ratio between the force per unit of surface that a layer of fluid exerts on the neighbors and the rate of deformation is constant.

2.3 Conservation equations

We call Fluid Mechanics the branch of mechanics that studies the movement of fluids, the forces that provoke them and the interaction of fluids with the environment that limits them. A fluid in motion can be described mathematically by the functions of velocity distribution and two thermodynamic magnitudes belonging to the fluid. In this way, using five magnitudes (the three components of velocity and for example, pressure and density), the state of the fluid is completely determined. The fundamental equations of fluid mechanics model the behavior of any type of flow by conserving two quantities, mass and momentum[1].

The following equations are necessary to understand the conservation of these magnitudes. These equations have been simplified under certain hypotheses assumed in a very common way by a large part of the scientific community. These hypotheses are:

- Mass continuity
- Negligible relativistic effects
- Absence of quantum effects
- Validity in inertial reference systems
- Interactions with negligible magnetic fields

A. Mass conservation

The law of mass conservation is fulfilled regardless of the nature of the fluid or the forces acting on it. This implies that throughout a fluid the mass is not destroyed or generated at any point. Mathematically this conservation law is expressed, in its differential form, as follows:

$$\frac{\partial \rho}{\partial t} + \nabla \cdot (\rho \vec{v}) = 0 \tag{2.1}$$

where ρ is the density of the fluid and $\vec{v}$ the velocity of the fluid at a point (x; y; z) of the space for a moment of time t. The first term of the previous expression represents the variation of mass per unit volume and unit of time at a certain point in space, and the second term refers to the variation of input and output velocity of mass in the system. The expression () is the so-called continuity equation, valid for all types of fluids. This expression appears in many fields of physics, such as Quantum Mechanics, Electromagnetic Theory, Relativistic Mechanics, etc.

B. Momentum conservation

The momentum is a vector physical quantity that, in the same way as mass, obeys the law of conservation. In the case of the fluids, the second Law of Newton affirms

"*the variation of motion per unit of time of a fluid mass is equal to that resulting from all the forces acting on that mass".*

The forces that act on a fluid are of two types, volume and surface forces. If we consider a control volume v_0 surrounded by a closed surface S_0, the volume forces are those that do not depend on the interaction of the fluid v_0 with the fluid that surrounds it and therefore affect the entire control volume equally. Gravitational force, electrical and magnetic forces are examples of these forces. In contrast, surface forces are forces that depend on the interaction of the fluid in v_0 with the fluid that surrounds it. They are forces that are exerted on the control volume v_0 through the surface S_0. Examples of these forces are the forces of pressure, viscosity or friction. Taking into account this the equation of motion is expressed as follows:

$$\rho \frac{D\,\vec{v}}{Dt} = \vec{f_v} + \vec{\nabla} \cdot \bar{\bar{\tau}} \tag{2.2}$$

where $\vec{f_v}$ denotes the volume forces acting on the fluid and $\bar{\bar{\tau}}$ is the tension tensor associated with the surface forces.

In this case the quotient x represents the variation over the time of the velocity of a fluid particle moving through space, it means, the axes of coordinates are located on each fluid particle. The description of the movement results from obtaining the trajectories that describe said particles. This way of describing fluids is called the Lagrangian description, one of the two formalisms that are commonly used to describe fluids macroscopically. The second of the formalisms is called Eulerian description, in which the axes are in fixed points of space, so in this case is the instantaneous description of the speed at each point what is obtained to represent the movement of the fluid.

A Eulerian point of view will be adopted, so we need to know the relationship between both descriptions to obtain the equation (2.2) so that the derivative of velocity refers to fixed points in space. The concept of a substantial derivative is the tool that allows us to move from one formalism to another. Intuitively, it can be postulated that this derivative reflects two different causes of change; on the one hand, the fact that speed may be changing over time locally; and on the other hand, the fact that the fluid particle may be moving in a field in which the velocity is not uniform.

The following equation expresses the changes in the velocity experienced by the fluid particle as it moves through the fluid field.

$$\frac{D\,\vec{v}}{Dt} = \frac{\partial \vec{v}}{\partial t} + (\vec{v} \cdot \vec{\nabla})\,\vec{v} \tag{2.3}$$

This equation is the definition [] of a substantial derivative of velocity. Substituting now in (2.2) we obtain the expression for the conservation of the moment of a viscous fluid referred to fixed points of the space.

$$\rho \left[\frac{\partial \vec{v}}{\partial t} + (\vec{v} \cdot \vec{\nabla})\,\vec{v} \right] = \vec{f_v} + \vec{\nabla} \cdot \bar{\bar{\tau}} \tag{2.4}$$

The stress tensor of (2.4) can be written as the sum of two terms, one representing the normal stress tensor produced by external forces on the surface of the system and the other the viscous stress tensor, that is,

$$\bar{\bar{\tau}} = -p\,\bar{\bar{I}} + \bar{\bar{\tau}}' \tag{2.5}$$

where p is the fluid pressure, $\bar{\bar{I}}$ is the unitary tensor and $\bar{\bar{\tau}}'$ the stress tensor of viscous stresses, related to the molecular transport of the quantity of movement. The tension tensor takes different forms depending on the type of fluid that is being considered. Below you will see the shape that the tensioners acquire when dealing with ideal fluids and with viscous fluids.

2.4 Ideal fluids

As already mentioned, an ideal fluid is a fluid in which the viscous forces are considered null. In these circumstances the only force acting on the fluid is the pressure, so that the total force on a certain volume is the integral of the pressure along the surface surrounding the volume. In this case the tension tensor (2.5) is a diagonal matrix with its three equal components p, so that by substituting (2.4) we come to the expression of the well-known Euler equation (dd), one of the fundamental equations of the fluid mechanics.

$$\rho\left[\frac{\partial\vec{v}}{\partial t} + (\vec{v}\cdot\vec{\nabla})\,\vec{v}\right] = \vec{\nabla}p \tag{2.6}$$

If we are in the presence of a gravitational field, the equation (2.6) must be modified, according to the equation (2.4), adding to the gradient of the pressure a term corresponding to the force exerted by the gravity on each element of volume.

$$\frac{\partial\vec{v}}{\partial t} + (\vec{v}\cdot\vec{\nabla})\,\vec{v} = \frac{\vec{\nabla}p}{\rho} + \vec{g} \tag{2.7}$$

2.5 Viscous fluids

It is now intended to obtain the equations of movement for a viscous fluid. For this, it is necessary to add to the tensor of tensions of an ideal fluid a term that reflects the transfer of viscous impulse, it means, the term $\bar{\bar{\tau}}'$ of the equation (2.5). The most general form of this tensor of rank two is represented as follows .

$$\bar{\bar{\tau}}'_{ij} = \eta \left[\frac{\partial v_j}{\partial x_i} + \frac{\partial v_i}{\partial x_j} - \frac{2}{3}\left(\vec{\nabla} \cdot \vec{v}\right)\bar{\bar{I}}\right] + \varsigma\left(\vec{\nabla} \cdot \vec{v}\right)\bar{I} \tag{2.8}$$

In this way, adding the divergence of the tensor (2.8) to the Euler equation, we obtain the general form of the equation of motion for a viscous fluid.

$$\rho\left[\frac{\partial \vec{v}}{\partial t} + \left(\vec{v} \cdot \vec{\nabla}\right)\vec{v}\right] = -\vec{\nabla}p + \vec{\nabla} \cdot \left\{\eta\left[\frac{\partial v_j}{\partial x_i} + \frac{\partial v_i}{\partial x_j} - \frac{2}{3}\left(\vec{\nabla} \cdot \vec{v}\right)\bar{\bar{I}}\right] + \varsigma\left(\vec{\nabla} \cdot \vec{v}\right)\bar{I}\right\} \tag{2.9}$$

The constants a and b are called first and second coefficients of viscosity, or dynamic viscosity and volumetric viscosity. These magnitudes are functions of pressure and temperature, so they are not constant throughout the fluid and cannot be pulled out of the divergence operator.
However, in most cases, the viscosity coefficients do not vary significantly along the fluid and can be considered constant, thus obtaining a simpler expression in vectoral form for the viscous fluids.

$$\rho\left[\frac{\partial \vec{v}}{\partial t} + \left(\vec{v} \cdot \vec{\nabla}\right)\vec{v}\right] = -\vec{\nabla}p + \eta\nabla^2\vec{v} + \left(\varsigma + \frac{1}{3}\eta\right)\vec{\nabla}\left(\vec{\nabla} \cdot \vec{v}\right) \tag{2.10}$$

If we are in a case in which we can consider the incompressible fluid, the density is constant along the same and the equation of continuity (2.1) is reduced $\vec{\nabla} \cdot \vec{v} = 0$. Thus, the last term in the second member of (2.10) is zero and we get the Navier-Stokes equation:

$$\rho\left[\frac{\partial \vec{v}}{\partial t} + \left(\vec{v} \cdot \vec{\nabla}\right)\vec{v}\right] = -\vec{\nabla}p + \eta\nabla^2\vec{v} \tag{2.11}$$

In this case, the stress tensor is reduced to a simple expression ($\bar{\bar{\tau}} = -\vec{\nabla}p + \eta\nabla^2\vec{v}$) that only depends on the dynamic viscosity η. However, it is common to find the written equations as a function of the coefficient $v = \frac{\eta}{\rho}$, called kinematic viscosity.

$$\frac{\partial \vec{v}}{\partial t} + \left(\vec{v} \cdot \vec{\nabla}\right)\vec{v} = -\frac{1}{\rho}\vec{\nabla}p + v\nabla^2\vec{v} \tag{2.12}$$

The Navier-Stokes equation (2.12) is a system of partial non-linear derivative equations formed by three equations, one for each direction of space. They are coupled to each other through pressure and speed.

2.6 Reynolds number

The Reynolds number is a parameter that appears in numerous problems of fluid mechanics because it allows to work with the Navier-Stokes equation in its dimensionless form. This number relates the kinematic viscosity *v* to, the main velocity of a problem v_0, and a third parameter related to the geometrical properties of the same, called characteristic length *l*[2].

- Viscosity $[\nu] = [m]^2/[s] = L^2\,T^{-1}$
- Length $[l] = [m] = L$
- Velocity $[v_0] = [m][s] = LT^{-1}$

With these three magnitudes a single dimensionless parameter is obtained, this combination, designated by Re, is what is known as the Reynolds number.

$$Re = \frac{v_0 l}{\nu} \tag{2.13}$$

The Reynolds number represents the ratio of viscous forces to those of inertia. High Reynolds numbers indicate that inertial forces are predominant versus viscous forces, and for high Reynolds numbers, Re > 4000, the flow will be turbulent. This implies that the movement of the fluid is very sensitive to any disturbance, which quickly expands to form swirls due to the irregular character of the flow. Conversely, for low Reynolds numbers, Re < 2000, the flow will be laminar, which means that any disturbance that the fluid can suffer will be easily damped and the layers of adjacent fluids will always be parallel. The flows that lie between these two values of Re belong to what is known as the zone of transition.

2.7 Simplified Equations

As previously mentioned, it is necessary to adapt the continuity and Navier-Stokes equations to our particular case and carry out additional simplifications, until we obtain the equations that have been implemented in the code. Below we will see in detail these simplifications:

- The physical properties of the fluid will be constant.

The direct consequence of this is that it will not be possible to study cases in which the fluid is compressible, it means, it assumes constant density. On the other hand, the viscosity of the fluid will also be constant, so that the simulation is limited to a range of temperatures in which the physical properties do not vary significantly.

- They are considered fluids in laminar regime.

This implies that turbulent flows could not be studied. Fluids are restricted to those with Reynolds numbers less than 2000.

- Work with Newtonian fluids.

At this point we eliminate all those fluids in which the relationship between the effort and the speed of deformation is not constant. For example, honey, heavy metals, blood and other "sticky" fluids will be excluded.

- They will be two-dimensional problems.

This is where we significantly limit the number of cases we can simulate. However, the essence of phenomenology is the same in two as in three dimensions and adding a third dimension complicates both the explanation and the visualization of results. In short, the wealth of description of the movement provided by the 3D case does not compensate the effort required in the programming and the higher computational cost of the simulations.

2.8 Boundary conditions

The general equations that govern the movement of fluids have been discussed in the previous sections. However, when the problem is reduced to a particular spatial domain, the information to obtain any particular solution from the system of equations (2.12) is insufficient. That is why it is essential to specify the boundary conditions that inform about the behavior of the fluid at the borders.

We will now review the most common boundary conditions for a viscous fluid, starting with the so-called non-slip condition. This condition is applied to the surface of solids and assumes that the relative velocity between the surface of the solid and the fluid finitely close to it is zero.

On the other hand, are the Dirichlet type boundary conditions. The information provided by this type of conditions is direct, that is, the value at the border of a generic variable ϕ is considered known, $\phi = f$. In the case of a fluid, this condition is generally applied to the incoming flow and implies that one of the components of the speed is known.

Finally, another of the most common boundary conditions are the so-called Newman conditions, which provide indirect information. In general, the value of the derivative of the variable ϕ in a normal direction n, $\partial \phi / \phi \, n = f$, at the border is known. Normally, these conditions are located in an area where the fluid is unidirectional and therefore there are no changes in the velocity component along that direction.

Throughout this chapter we have seen in detail the fundamentals and concepts necessary to understand the phenomenology of fluid mechanics. The next step is to establish the fundamentals of computational fluid mechanics to be able to translate the equations that intervene in each problem to the computational language. Therefore, in the next chapter the necessary steps to carry out said translation will be explained.

2.9 Summary chapter

Throughout this chapter we have seen different concepts that will be of great help later in the realization of this work.
It starts with the classification of fluids which we have classified into 4 groups in a general manner that are the following;

- Steady - Non-steady
- Incompressible - compressible
- Ideal - Viscous
- Newtonian

Then it is passed to the conservation equations and here also has been classified in two parts, the conservation of the mass and the momentum. These two hypotheses are a fundamental part when it comes to simplifying the Navier-Stokes equations.

One of the parameters that will be used during the realization of this work is undoubtedly the number of Reynolds, this parameter helps me to distinguish in which study regime I am working this can be laminated as turbulent. Finally, the boundary equations, these equations tell me how I have to behave at the border or the problem.

With the description of these concepts we can now enter more fully to the realization of this work which aims to study the Navier-Stokes equations.

3.The convection-diffusion equation

3.1Introduction

When a fluid plays a significant role in the problem, the effects of convection must be considered. This means that a transport of the general properties takes place by means of two different phenomena: the diffusion, related to the molecular movement, and the convection, related to the macroscopic movement. As shown in the transport equation, derived from the Reynolds Transport Theorem, which represents the flow balance in the control volume.

$$\frac{\partial \rho \phi}{\partial t} + \nabla \cdot (\rho \vec{v} \phi) = \nabla \cdot (\Gamma \nabla \phi) + S \tag{3.1}$$

The property to be evaluated is the phi value (ϕ). On the left side of the equation above there are two terms, the first one is the accumulative term that represents the general property ϕ in the control volume and the second one is the flux by convection. On the right side another two terms, the first one is the diffusive flux and the second one is the source term that corresponds to an internal or external source that could variance the general property ϕ in the control volume. The conduction-diffusion equation and the problems related to it assume the velocity field known. Note that the above equation will be used to solve static problems by means of the transient nature of the equation in order to get the solution to converge until it is static.

3.2 Discretization of the convection-diffusion equation

Considering the following governing equations, corresponding to the Reynolds Equation of Transportation and the Equation of Continuity[3].

$$\frac{\partial \rho}{\partial t} + \nabla \cdot (\rho \vec{v}) = 0 \tag{3.2}$$

Using a rectangular finite volume and integrating the first equation and making use of the Gauss-Ostrogradsky theorem, we obtain the following expression:

$$\frac{(\rho\phi)_P^{n+1} - (\rho\phi)_P^n}{\Delta t}\Delta x\Delta y + [(\rho u\phi)_e^{n+1} - (\rho u\phi)_w^{n+1}]\Delta y + [(\rho v\phi)_n^{n+1} - (\rho v\phi)_s^{n+1}]\Delta x = \left[\left(\Gamma \frac{\partial \phi}{\partial x}\right)_e^{n+1} - \left(\Gamma \frac{\partial \phi}{\partial x}\right)_w^{n+1}\right]\Delta y + \left[\left(\Gamma \frac{\partial \phi}{\partial x}\right)_n^{n+1} - \left(\Gamma \frac{\partial \phi}{\partial x}\right)_s^{n+1}\right]\Delta x + S_p^{n+1}\Delta x\Delta y \tag{3.3}$$

It's convenience to simplify the equation above to obtain discrete equations for convection-diffusion problems.

Convective term

$$F_e = \rho u_e \tag{3.4}$$

$$F_w = \rho u_w \tag{3.5}$$

$$F_n = \rho v_n \tag{3.6}$$

$$F_s = \rho v_s \tag{3.7}$$

Diffusive term

$$D_e = \frac{\Gamma_e}{\partial x_e} \tag{3.8}$$

$$D_w = \frac{\Gamma_w}{\partial x_w} \tag{3.9}$$

$$D_n = \frac{\Gamma_n}{\partial y_n} \tag{3.10}$$

$$D_s = \frac{\Gamma_s}{\partial y_s} \tag{3.11}$$

With these new expressions, the conservation equations for mass and momentum can be rewritten as:

$$\frac{(\rho\phi)_P^{n+1}-(\rho\phi)_P^n}{\Delta t}\Delta x\Delta y + [(F_e\phi)_e^{n+1} - (F_w\phi)_w^{n+1}]\Delta y + [(F_n\phi)_n^{n+1} - (F_s\phi)_s^{n+1}]\Delta x = \left[D_e(\phi_e - \phi_p)^{n+1} - D_w(\phi_p - \phi_w)^{n+1}\right]\Delta y + \left[D_n(\phi_n - \phi_p)^{n+1} - D_s(\phi_p - \phi_s)^{n+1}\right]\Delta x + S_p^{n+1}\Delta x\Delta y \tag{3.12}$$

Introducing the equation of continuity in the formulation, this will give greater stability to the problem, compliance with the continuity implies that there will be no physical inconsistencies in the solution. Therefore, introducing these new terms in the previous equations the equation below is obtained.

$$\frac{(\rho\phi)_P^{n+1} - (\rho\phi)_P^n}{\Delta t}\Delta x\Delta y + [(J_e - J_w)^{n+1} - (J_n - J_s)^{n+1}] - \phi_P^{n+1}[(F_e - F_w)^{n+1} - (F_n - F_s)^{n+1}] = S_p^{n+1}\Delta x\Delta y \quad (3.13)$$

It is useful to consider a total flux *J* that is made up of convection flux and diffusion flux. The table below shows the total flux.

$$J_e = [F_e - D_e(\phi_E - \phi_P)]\Delta y \quad (3.14)$$

$$J_w = [F_w - D_w(\phi_P - \phi_W)]\Delta y \quad (3.15)$$

$$J_n = [F_n - D_n(\phi_N - \phi_P)]\Delta x \quad (3.16)$$

$$J_s = [F_s - D_s(\phi_P - \phi_S)]\Delta x \quad (3.17)$$

3.3 Grid

The partial differential equations that govern fluid flow and heat transfer are not usually amenable to analytical solutions, except for very simple cases. Therefore, in order to analyze fluid flows, flow domains are split into smaller subdomains. The governing equations are then discretized and solved inside each of these subdomains. Typically, one of three methods are used to solve the approximate version of the system of equations: finite volumes, finite elements, or finite differences. Care must be taken to ensure proper continuity of solution across the common interfaces between two subdomains, so that the approximate solutions inside various portions can be put together to give a complete picture of fluid flow in the entire domain. The subdomains are often called elements or cells, and the collection of all elements or cells is called a mesh or grid[4].

There are different options according to the study case, some of the available options are the following:

- Structured grid
- Block-structured grid
- Unstructured grids

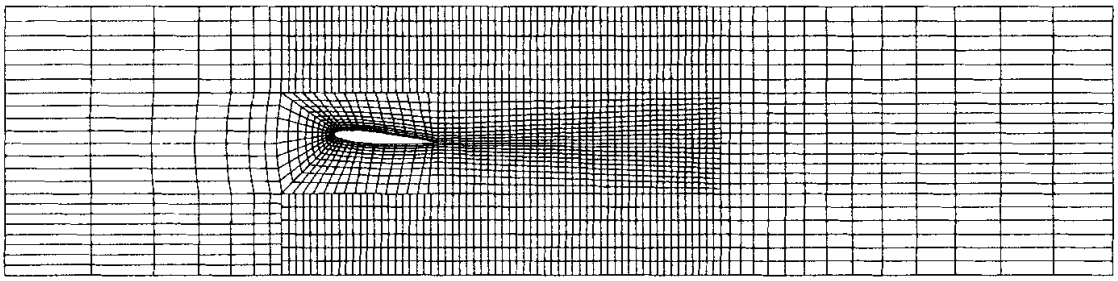

Figure 3: Example of a 2D block-structured grid, designed for calculation of flow around a hydrofoil under a water surface

3.3.1 Finite volume Method

The calculation domain is divided into several nonoverlapping control volumes such that there is one control volume surrounding each grid point. The differential equation is integrated over each control volume. Piecewise profiles expressing the variation of ϕ between the grid points are used to evaluate the required integrals. The result is the discretization equation containing the values of ϕ for a group of grid points.

A resolution model of Navier-Stokes differential equations has been chosen for finite control volumes for the development of this work, being of particular interest the type of mesh used. This type of meshing can be obtained by two procedures, chosen according to the practical application:

- **Centered faces**: It consists of placing the nodes (study points of the mesh) in the desired positions, and then generating a volume of control around the node.
- **Centered nodes**: First the control volumes must be generated within the domain, and once they are established, the node is placed in the center of the volume.

In addition, the obtained discretization equations must comply with the four basic rules shown below:

a) Consistency in the faces of the control volume. When one face is in contact with two adjacent control volumes, the flow through the faces must be represented by the same expression of discretization in the two control volumes.

b) Positive coefficients. The increase in the value of a point of the mesh, with the other unalterable conditions, must lead to the increase of the value to the neighboring point in the mesh.

c) The linearized internal sources must have a negative slope so that the coefficient of the study point, known as a_P, is not negative.

d) The value of the coefficient of the study point, a_P, must be equal to the sum of the coefficients of the neighboring points.

With these conditions, doing a study in two dimensions, we obtain a discretized equation, of the form:

$$a_P\phi_P = a_N\phi_N + a_S\phi_S + a_E\phi_E + a_W\phi_W + b_P$$

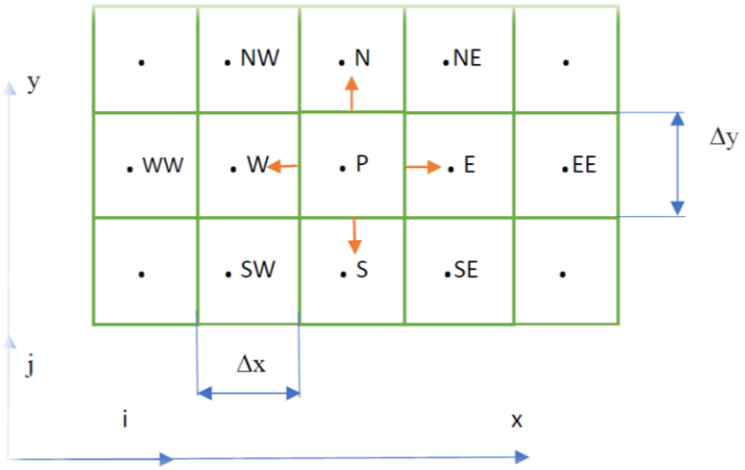

Figure 4: A typical CV and the notation used for a Cartesian 2D grid.

3.4 Temporal Discretization

For the development of the calculations we must specify the temporary schemes that are going to be used, since the final formulation of the method depends on them. There are numerous temporary schemes, but roughly they can be divided into two groups:

- Explicit schemes

The explicit schemes are those that assume that the values of the variables in the new time step depend only on the value of the variable in the previous instant. They are schemes that approximate the new values from the calculated ones, so they require a lower computational cost, but at the same time the stability of them is also lower.

- Implicit schemes

In the implicit schemes the value of the variables in the new time step is no longer approaching, it is calculated precisely from both the previous and the next instant. The computational cost in this case is much higher in each iteration, but they have the advantage that the stability of the method is very high.

3.5 Numerical Schemes

Numerical results will only be physically realistic when the discretization scheme has certain fundamental properties. In some cases of study, it will be necessary to evaluate the properties and their corresponding gradients in the faces of the control volume, being necessary the use of resolution schemes that relate the variable in the face of the control volume with the values of the known nodes[5].

- Fundamental properties:

1. ***Conservativeness;*** The equations are based of mass conservation. To ensure a conservation of ϕ for the whole solution domain, the flux leaving a control volume across a certain face must be equal to the flux entering the adjacent control volume through the same face. Therefore, all schemes used should be conservativeness.

2. ***Boundedness;*** The discretized equations at each nodal point represent a set of algebraic equations that needs to be solved. Normally iterative numerical techniques are used to solve large equation sets. These methods start the solution process from a guessed distribution of the variable ϕ and perform successive updates until a converged solution is obtained.

3. ***Transportiveness;*** It is very important that the relationship between the directionality of influencing and the flow direction, known as the transportiveness, is borne out in the discretization scheme. In order to understand these phenomena, the Peclet number is introduced. According to the Peclet number the internal node P is influenced by the west or east node, therefore it expressed the flow direction.

$$P_e = \frac{F}{D} \tag{3.18}$$

No convection and pure diffusion $(P_e --> 0)$
No diffusion and pure convection $(P_e --> \infty)$

The figure below shows the convectional positive fluxes in the control volume $F > 0$.

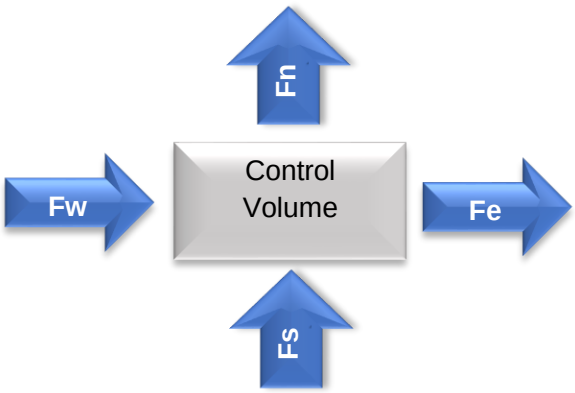

Figure 5: Positive Volume Fluxes.

- **Low order schemes**

a) Upwind Difference Scheme (UDS)

The upwind differencing scheme utilizes consistent expressions to calculate fluxes through cell faces; therefore, it can be easily shown that the formulation is conservative. The coefficients of the discretized equation are always positive and satisfy the requirements for boundedness[6].

PHI VALUE	MASS FLOW > 0	MASS FLOW < 0
Φ_n	Φ_P	Φ_N
Φ_s	Φ_S	Φ_P
Φ_e	Φ_P	Φ_E
Φ_w	Φ_W	Φ_P

Table 1: UpWind difference Scheme Value accordinf to the mass flow.

The scheme is based on the backward differencing formula, so the accuracy is only first-order based on the Taylor series truncation error. A major drawback of the scheme is that it produces erroneous results when the flow is not aligned with the grid lines.

b) Central Difference Scheme (CDS)

The central differencing scheme is one of the schemes used to solve the integrated convection-diffusion equation and to calculate the transported property ϕ at the east and west faces.

$$\phi_e = \frac{\phi_E + \phi_P}{2} \tag{3.19}$$

$$\phi_n = \frac{\phi_N + \phi_P}{2} \tag{3.20}$$

$$\phi_w = \frac{\phi_P + \phi_W}{2} \tag{3.21}$$

$$\phi_s = \frac{\phi_P + \phi_S}{2} \tag{3.22}$$

If Pe is greater than 2 the east coefficient will be negative. This violates one of the requirements for boundedness and may lead to physically impossible solutions.

c) Hybrid Different Scheme (HDS)

The hybrid differencing scheme is based on a combination of central and upwind differencing schemes. The central differencing scheme, which is second order accurate, is employed for small Peclet numbers (Pe < 2) and the upwind scheme, which is first order accurate but accounts for transportiveness, is employed for large Peclet numbers (Pe ≥2).
The hybrid difference scheme exploits the favorable properties of the upwind and central differencing schemes. The disadvantage is that the accuracy in terms of Taylor series truncation error is only first-order.

d) Exponential Difference Scheme (EDS)

The evaluation of the variable at the cell face comes from the exact solution of the convection-diffusion equation in one-dimensional case, null source term and steady problem. As this scheme is more accurate, it also takes more computational efforts and time.

e) Power Law Scheme (PLS)

Evaluates the variable at the cell face using an approximation of *EDS* scheme by a polynomial of fifth degree. It is simpler than *EDS*, but, even so, it takes more computational efforts than *UDS*, *CDS* or *HDS* schemes.

Now introducing one of the schemes above in the discretized equations of convection-diffusion, the following expression is obtained.

$$a_P\phi_P^{n+1} = a_N\phi_N^{n+1} + a_S\phi_S^{n+1} + a_E\phi_E^{n+1} + a_W\phi_W^{n+1} + b_P \tag{3.23}$$

$a_N = D_N \cdot A(P_N) + max(-F_N, 0)$		$F_n = (\rho v)_n \Delta x$	$D_n = \frac{\Gamma_n \Delta x}{(\delta y)_n}$
$a_S = D_S \cdot A(P_S) + max(F_S, 0)$		$F_s = (\rho v)_s \Delta x$	$D_s = \frac{\Gamma_s \Delta x}{(\delta y)_s}$
$a_E = D_E \cdot A(P_E) + max(-F_E, 0)$		$F_e = (\rho u)_e \Delta y$	$D_e = \frac{\Gamma_e \Delta y}{(\delta y)_e}$
$a_W = D_W \cdot A(P_W) + max(F_W, 0)$		$F_w = (\rho u)_w \Delta y$	$D_w = \frac{\Gamma_w \Delta y}{(\delta y)_w}$
$a_P = a_P + a_P + a_P + a_P + a_P + b_P$			
$b_P = \rho_P^n \cdot \frac{\Delta x \Delta y}{\Delta t} \cdot \phi_P^n$			

Table 2: Final discretized form of convection-diffusion equation.

Numerical Scheme	*A(P)*
UDS	*1*
CDS	*1 – 0.5 (| P |)*
HDS	*max (0, 1 – 0.5 (| P |)*
EDS	*|P| / (e $^{|P|}$ - 1)*
PLDS	*max (0, (1 – 0.5 (| P |)^5)*

Table 3: Value of P for each Numerical Scheme.

- **High order schemes**

The use of upwind quantities ensures that the schemes are very stable and obey the transportiveness requirements, but the first order accuracy makes them prone to numerical diffusion errors. Such errors can be minimized by employing higher-order discretization. The higher-order schemes involve more neighbor points and reduce the discretization errors by bringing in a wider influence. By adding a new term into the general formulation that acts like a source the new equation is written as follows[7].

$$a_P\phi_P^{n+1} = a_N\phi_N^{n+1} + a_S\phi_S^{n+1} + a_E\phi_E^{n+1} + a_W\phi_W^{n+1} + b_P + b_{de} \tag{3.24}$$

$$b_{de} = F_n(\phi_n^{UDS} - \phi_n^{HS}) - F_s(\phi_s^{UDS} - \phi_s^{HS}) + F_e(\phi_e^{UDS} - \phi_e^{HS}) - F_w(\phi_w^{UDS} - \phi_w^{HS}) \tag{3.25}$$

$$\phi_n^{UDS} \text{ --> } Upwind\ difference\ scheme$$
$$\phi_n^{HS} \text{ --> } High\ resolution\ scheme$$

To compute the high-resolution scheme a normalized variable formulation is introduced. The proposed scheme is formulated based on the normalized variable. Considering face f of a control volume defining ϕ_U, ϕ_D, ϕ_C, and ϕ_f as the upstream (U), downstream (D), central nodal values (C), and face value (f) for each cell face, the normalized value is defined as

$$\bar{\phi} = \frac{\phi - \phi_U}{\phi_D - \phi_U} \tag{3.26}$$

Note that with this normalization $\bar{\phi}_D = 1$ and $\bar{\phi}_U = 0$. The use of the normalized variables simplifies the definition of the functional relationships of HR schemes and will be helpful in defining the conditions the functional relationships should satisfy in order to have the property of boundedness and stability.

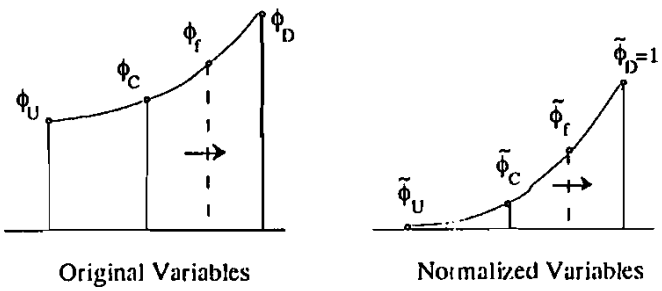

Figure 6: Original and Normalized variables

a) Upwind Second Order

For this case it uses again the value of the variable in the central node of the control volume from where the flow comes, but it also considers the value of the variable in the previous node of the flow direction. The scheme consists of a lineal extrapolation between ϕ_C and ϕ_U. The value at the cell face is shown in the equation below.

$$\phi_{face} = \frac{3}{2}\phi_C + \frac{1}{2}\phi_U \tag{3.27}$$

North face

$$\phi_n = \frac{3}{2}\phi_P + \frac{1}{2}\phi_S \tag{3.28}$$

South face

$$\phi_s = \frac{3}{2}\phi_S + \frac{1}{2}\phi_{SS} \tag{3.29}$$

West face

$$\phi_e = \frac{3}{2}\phi_P + \frac{1}{2}\phi_W \tag{3.30}$$

East face

$$\phi_w = \frac{3}{2}\phi_W + \frac{1}{2}\phi_{WW} \tag{3.31}$$

b) Quick Scheme

This scheme uses a three-point upstream quadratic interpolation for cell face values. The face value of ϕ is obtained from a quadratic function passing through two nodes (on each side of the face) and one node on the upstream. The value at each cell face is shown below.

$$\phi_{face} = \frac{6}{8}\phi_C + \frac{3}{8}\phi_D - \frac{1}{8}\phi_U \tag{3.32}$$

North face

$$\phi_n = \frac{6}{8}\phi_P + \frac{3}{8}\phi_N - \frac{1}{8}\phi_S \tag{3.33}$$

South face

$$\phi_s = \frac{6}{8}\phi_S + \frac{3}{8}\phi_P - \frac{1}{8}\phi_{SS} \tag{3.34}$$

West face

$$\phi_e = \frac{6}{8}\phi_P + \frac{3}{8}\phi_E - \frac{1}{8}\phi_W \tag{3.35}$$

East face

$$\phi_w = \frac{6}{8}\phi_W + \frac{3}{8}\phi_P - \frac{1}{8}\phi_{WW} \tag{3.36}$$

3.6 Solvers

Once we have the discretized study equations and particularized for the given geometry and the boundary conditions, what is obtained is a matrix of algebraic equations that encompasses all the study points of the domain, of the form $A \cdot x = b$, where both A and b are known values.

Although initially it may seem easy to solve the system to find x (our unknown), the inversion of matrix A is not trivial and therefore it is necessary to find a tool that simplifies the calculations. These tools are the resolution algorithms, better known as solvers, which are divided into two large groups: direct and iterative [8].

- Direct solvers

The direct solvers are those that directly solve the study equations, achieving only with a calculation process the value of the variables. They are solvers difficult to program but fast in execution, which saves calculation time. Among them, the TDMA or Tridiagonal Matrix Algorithm stands out, a very useful and fast method when matrix A only contains three adjacent

diagonals. This particularity makes their application cases are limited, since it is not always possible for the matrix to contain only three diagonals, however, when it is the case, it is the most practical method.

The tridiagonal system of the equations may be written as:

$$a_i x_i + b_i x_{i-1} + c_i x_{i+1} = d_i \tag{3.37}$$

Written in the matrix form,

$$\begin{bmatrix} a_1 & c_1 & & & & 0 \\ b_2 & a_2 & c_2 & & & \\ & b_3 & a_3 & c_3 & & \\ & & \ddots & \ddots & \ddots & \\ & & & b_{n-1} & a_{n-1} & c_{n-1} \\ 0 & & & & b_n & a_n \end{bmatrix} \begin{bmatrix} x_1 \\ x_2 \\ \vdots \\ \vdots \\ x_{n-1} \\ x_n \end{bmatrix} \begin{bmatrix} d_1 \\ d_2 \\ \vdots \\ \vdots \\ d_{n-1} \\ d_n \end{bmatrix} \tag{3.38}$$

The method consists in directly solve the written matrix:

$$P_i = \frac{c_i}{a_i - b_i \cdot P_{i-1}} \tag{3.39}$$

$$R_i = \frac{d_i + b_i \cdot R_{i-1}}{a_i - b_i \cdot P_{i-1}} \tag{3.40}$$

And finally, the concurrency formulae to find the direct solution for each x_i is,

$$x_i = P_i \cdot x_{i+1} + R_i \tag{3.41}$$

The way to solve is, first, calculate the values of P_i and R_i for each node in ascendant. Notice that for the first node $i = 1$: $P_1 = \frac{c_1}{a_1}$ and $R_1 = \frac{d_1}{a_1}$. Then, to find the x_i values, it is needed to set the $x_n = R_n$, and with the equation (3.41) find the rest of the values from $i=n-1$ to $i=1$(descending order)

- Iterative solvers

The iterative solvers are based on the concept of trial and error. The resolution starts with a random value, and based on repeating the calculations, using a convergence criterion, the final value of the variable is reached. Among them Gauss-Seidel stands out, one of the simplest algorithms of this type. Its operating principle consists of assuming an initial solution value for each node, performing an iteration and checking the results for each node with the assumed or last calculated value, until the difference meets the chosen convergence criterion.

The Gauss-Seidel algorithm is a iterative method that solves the values of x point by point in the following manner in the equation (3.42), for each i = 1, 2,…n.

$$x_i^{k+1} = \frac{1}{a_{ij}}\left(-\sum_{j<i} a_{ij}x_j^{k+1} - \sum_{j>i} a_{ij}x_j^{k} + b_i\right) \tag{3.42}$$

The new values of x_i^{k+1} are used as soon as they are known. For example, first it is computed the value of x_1^{k+1}, and once this is computed it is used in the second equation to calculate the new x_2^{k+1}, and so on.

As it is and iterative method when the x_i^{k+1} values are fond for all the domain values of I it is needed to check (for each value of I from 1 to n) if the method has converged, with the next expression.

$$\left\| x_i^{k+1} - x_i^{k} \right\| < \delta$$

Within the iterative solvers also highlights the Line-By-Line, which is a combination of Gauss-Seidel with TDMA. When matrix A is not tri-diagonal, there is a way to force it to be by including the values of the variables needed in the independent term. In this way we get a new matrix A that is tri-diagonal, on which we can apply TDMA. However, since the matrix is not the original one, an iterative process must be carried out, using Gauss-Seidel to obtain the final values of the system.

3.7 Summary chapter

During this chapter we have seen the convection-diffusion equations in their incompressible form. we have seen the Navier-Stokes equation in its general form to later discretize it. the equation has been discretized in one convective part and the other diffusive. Using these expressions and following the hypothesis of conservation and momentum has reached a final expression which will be the key to face this work.

The spatial discretization has been analyzed, that for this work we will use the FVM (Finite Volume Method). Three types of meshes can be classified in their general form;

- Structured grid
- Block-structured grid
- Unstructured grids

Another fundamental part of this chapter has been the temporal discretization, we have seen two types of discretization which later will be of great help when considering the resolution of problems, The numerical schemes which we have classified into two types, First order scheme and High Resolution Scheme, have been seen in detail how to implement these types of schemes and which is the most convenient when developing a case study. Finally, the Solvers necessary for the development of this project, these solvers are classified into two major categories;

- Iterative Solver
- Direct Solver

Now we turn to the next chapter which aims to develop codes in MATLAB to study and analyze different cases of computational fluid dynamics.

4 Problems Convection-Diffusion Test problems

4.1 Introduction

The purpose of this chapter is to have a familiarity with the cases of convection-diffusion which with the mathematical formulation seen in chapter two and the discretization of the Navier-Stokes equations in chapter three we can now study three cases that are the following;

- A Two- Dimensional Transient Conduction Problem
- Diagonal Flow Problem
- Smith-Hutton Problem

The first case the heat transfer by conduction presents an interesting starting point for the study of the formulation of the Navier-Stokes equations, since the physical processes involved are easy to understand and do not present a great technical difficulty

The heat transfer has a negative gradient. This fact can be observed in the following equation, where the heat flow is expressed as a function of temperature, this being proportional to the gradient by means of a constant, λ, known as thermal conductivity.

$$q = -\lambda \frac{\partial T}{\partial x} \tag{4.1}$$

The other two cases are the Diagonal Flow and Smith-Hutton, the first is based on a diagonal flow and the second on a solenoid flow confined in a rectangle. For these cases of studies different simulations will be made to different Reynolds numbers as well as with different mesh density and numerical schemes.

For the resolution of these cases, two types of Solver have been proposed, for the case of Heat Transfer by conduction the solver that we will use is the Line by Line and for the two following cases the Point by Point. Next, the case studies.

4.2 A Two- Dimensional Transient Conduction Problem

This problem consists in a very long rod composed of four different materials, as it can be seen in the figure 7. As the draw is not a scale in the table 10 the coordinates of the points $p1$, $p2$ and $p3$ are given. The properties of each one of the four materials are given in table 9, and boundary conditions can be found in the table 11. Furthermore, the initial temperature field is known, and is T=8.00 $°C$.

The objective of this exercise is to obtain the value of the temperatures in each point of the domain, for each instant of time. The temporal evolution of the temperature of the domain points (0.65, 0.56) and (0.74, 0.72) will be studied to facilitate the graphic representation of the results.

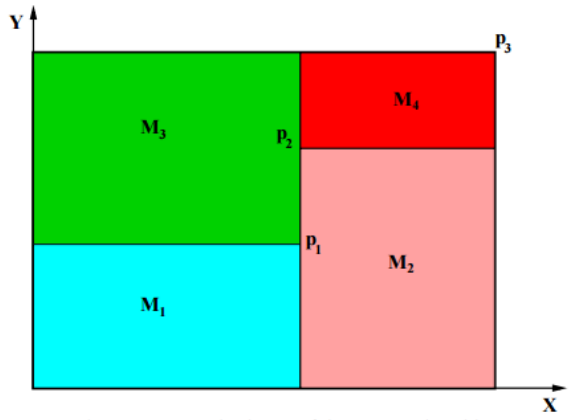

Figure 7: The two-transient conduction problem scheme[9].

	ρ[Kg/m^3]	c_p[J/KgK]	λ[W/mK]
M1	1500.00	750.00	170.00
M2	1600.00	770.00	140.00
M3	1900.00	810.00	200.00
M4	2500.00	930.00	140.00

Table 4: Transient conduction problem properties

	x[m]	*y*[m]
P1	0.50	0.40
P2	0.50	0.70
P2	1.10	0.80

Table 5: Coordinates of the problem

Cavity Wall	Boundary Conditions
Bottom	*Isotherm T= 23 ^{0}C*
Top	*Uniform Q_{flow} = 60 W/m length*
Left	*In contact with a fluid T_g = 33^{0}C and a heat transfer coefficient 9 W/m^{2}K*
Right	*Uniform temperature T=8 + 0.005 ·t ^{0}C*

Table 6: Boundary conditions of transient conduction problem

- **Assumptions**

For the resolution of this exercise, the following hypotheses must have been formulated:

1. Constant thermophysical properties.
2. Transient study of the equations.
3. The calculation of the equations will be done for times from 0 to 10000, with a temporary increase of 1s.
4. Two-dimensional study of the case, so that the contribution of depth will not be considered in the equations.
5. An implicit resolution scheme will be used.

Governing Equations

For the resolution of this exercise, a discretization of centered nodes has been chosen, generating two-dimensional control volumes, in which the node where the temperature is evaluated is in the center. Using this type of discretization, it is necessary that in the generated control volumes none appear with different materials, so that a horizontal division and two verticals have been made taking advantage of the limits imposed by each material, thus generating a different mesh density for each one of them. When evaluating the thermal conductivity in the faces between nodes, a harmonic mean of the value will be made.

In this way, for two nodes with equal thermal conductivity, the harmonic mean will give this value, while if the nodes are of different materials a weighted value will be obtained with the size of each control volume.

This is a case of pure conduction and constant physical properties. Therefore, the energy equation is the only equation which will be used to obtain the temperature field.

$$\frac{\partial T}{\partial t} = \frac{\lambda}{\rho c_p} \nabla^2 T \tag{4.2}$$

Numerical Methods

For the time integration a full implicit method will be used for this problem, integrating the equation (4.2) the following term is obtained.

$$\int_{t^n}^{t^{n+1}} \frac{\partial T}{\partial t} dt = T^{n+1} - T^n = \int_{t^n}^{t^{n+1}} \frac{\lambda}{\rho c_p} \nabla^2 T \, dt \approx \frac{\lambda}{\rho c_p} \nabla^2 T^{n+1} \Delta t \tag{4.3}$$

$$\frac{T^{n+1} - T^n}{\Delta t} = \frac{\lambda}{\rho c_p} \nabla^2 T^{n+1} \tag{4.4}$$

To obtain the temperature field for each time step, the equation must be integrated over the whole domain. First the transient term will be integrated and then the diffusive term.

$$\int_{\Omega} \frac{T^{n+1} - T^{n}}{\Delta t}\, d\Omega \approx \frac{T^{n+1} - T^{n}}{\Delta t}\, \Delta x \Delta y \tag{4.5}$$

$$\int_{\Omega} \nabla^2 T^{n+1}\, d\Omega = \int_{\Omega} \nabla \cdot (\nabla T^{n+1}) d\Omega = \int_{\partial\Omega} \nabla T^{n+1} \cdot \hat{n} dS =$$
$$\left(\frac{T_E^{n+1} - T_P^{n+1}}{\Delta x_{d_e}} - \frac{T_P^{n+1} - T_W^{n+1}}{\Delta x_{d_w}}\right)\Delta y + \left(\frac{T_N^{n+1} - T_P^{n+1}}{\Delta y_{d_n}} - \frac{T_P^{n+1} - T_S^{n+1}}{\Delta y_{d_s}}\right)\Delta x \tag{4.6}$$

To solve the problem, we must arrive at the following equation.

$$a_P T_P^{n+1} = a_N T_N^{n+1} + a_S T_S^{n+1} + a_E T_E^{n+1} + a_W T_W^{n+1} + b_P \tag{4.7}$$

West nodes

$$a'_W = 0 \tag{4.8}$$

$$a'_p = a_p + \frac{a_W \lambda_w}{\Delta x_{d_w} + \lambda_w} \tag{4.9}$$

$$b'_p = b_p - \frac{a_W \Delta x T_g}{\Delta x_{d_w} + \lambda_w} \tag{4.10}$$

North nodes

$$a'_N = 0 \tag{4.11}$$

$$a'_p = a_N + a_N \tag{4.12}$$

$$b'_p = b_p - a_N \frac{q_{top} \Delta y_{d_n}}{\lambda_n} \tag{4.13}$$

East nodes

$$a'_E = 0 \tag{4.14}$$

$$b'_p = b_p - a_E T_{right} \tag{4.15}$$

South nodes

$$a'_S = 0 \tag{4.16}$$

$$b'_p = b_p - a_S T_{bottom} \tag{4.17}$$

Inner nodes

$$a_N = -\frac{\lambda_n}{\rho c_p}\frac{\Delta x}{\Delta y_{d_n}} \tag{4.18}$$

$$a_S = -\frac{\lambda_S}{\rho c_p}\frac{\Delta x}{\Delta y_{d_s}} \tag{4.19}$$

$$a_E = -\frac{\lambda_e}{\rho c_p}\frac{\Delta y}{\Delta y_{d_e}} \tag{4.20}$$

$$a_W = -\frac{\lambda_w}{\rho c_p}\frac{\Delta y}{\Delta y_{d_w}} \tag{4.21}$$

$$b_p = T_p^n \frac{\Delta x \Delta y}{\Delta t} \tag{4.22}$$

Results

Below we can see the results obtained by developed code. The precision obtained would be greater with a denser meshing, but an increase in the number of nodes affects a greater time and calculation effort.

The temperature map for an instant of time of 5000 and 10000 seconds can be appreciated in the graph below. Analyzing the images, in the lower wall the temperature remains constant over time and as the temperature of the right wall increases proportionally to the time elapsed.

Considering the possible calculation errors due to the precision obtained with the work mesh, it can be seen how the results that have been obtained are quite similar to the reference by the CTTC (Centre Tecnologic Heat Transfer)

It can be concluded that the number of chosen nodes is enough to obtain an accurate solution. This solution has a physical meaning since the right side is at approximately 33ºC and the bottom boundary at 23ºC. Inside the domain, a temperature degradation can be observed from a temperature of about 33ºC on the right boundary to a temperature of 23ºC on the left and bottom boundaries.

Time: 5000 seconds

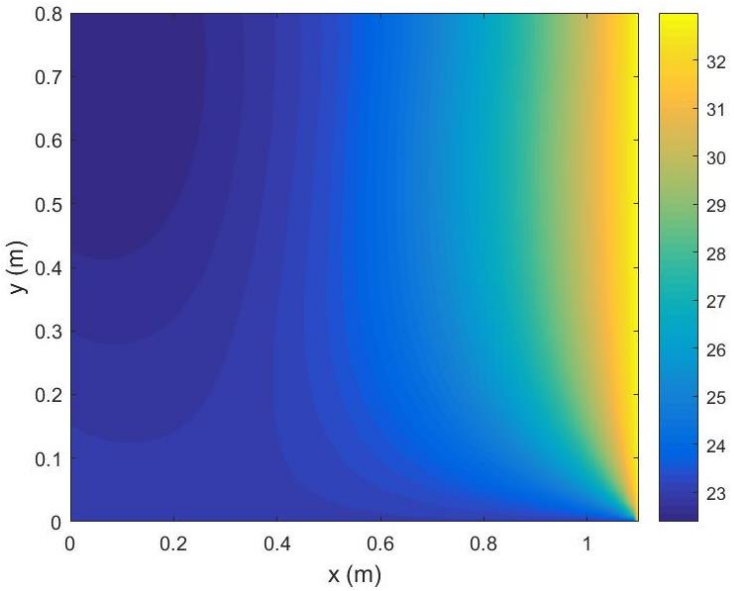

Figure 8: Temperature at 5000 seconds

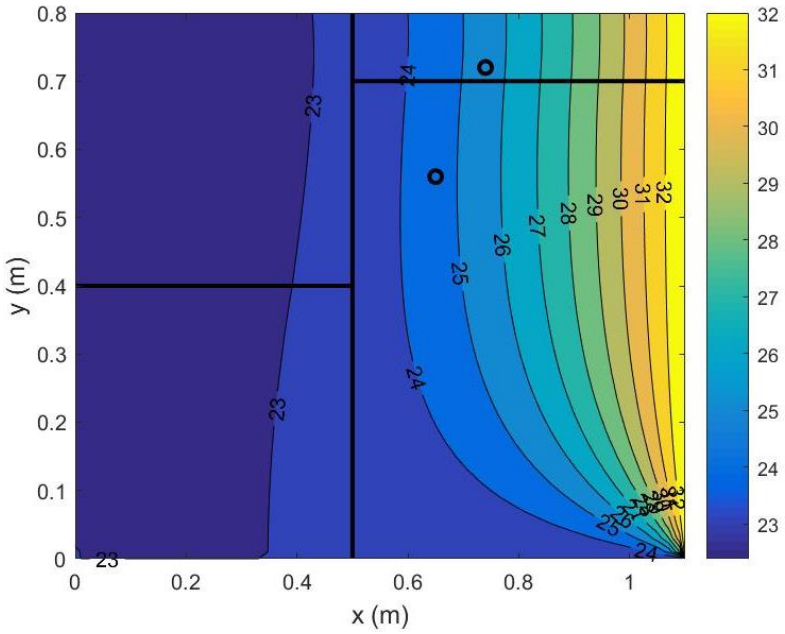

Figure 9: Temperatures at 5000 seconds with the two Points requested.

Time: 10000 seconds

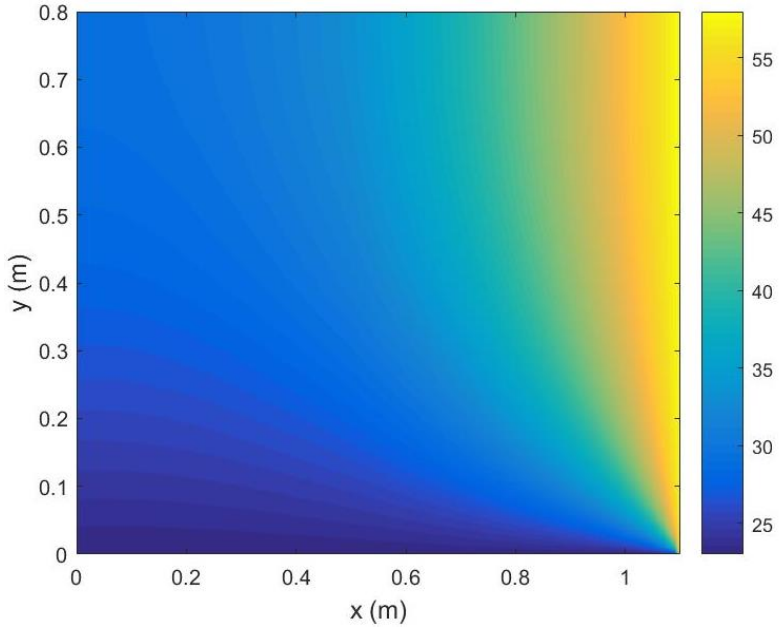

Figure 10: Temperature at 10000 seconds

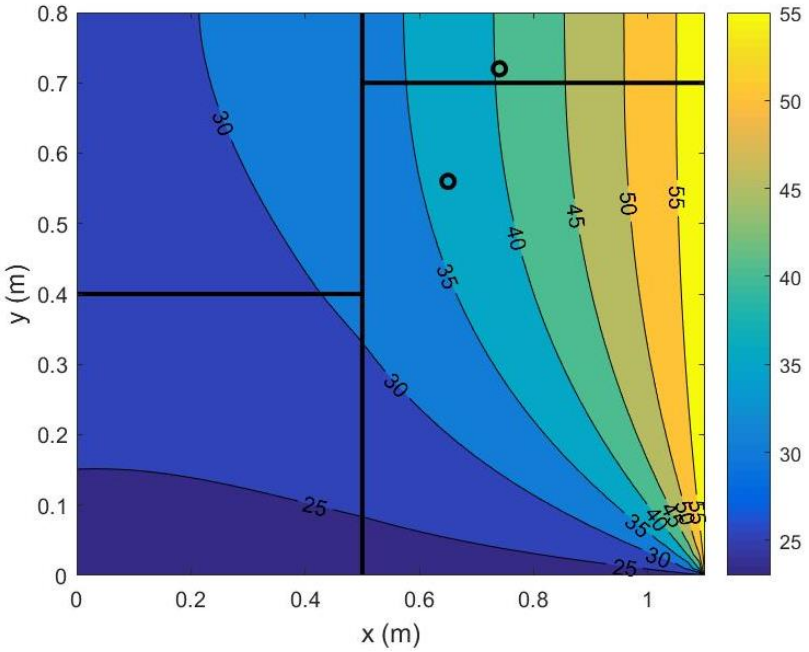

Figure 11: Temperature at 10000 seconds with the two Points requested.

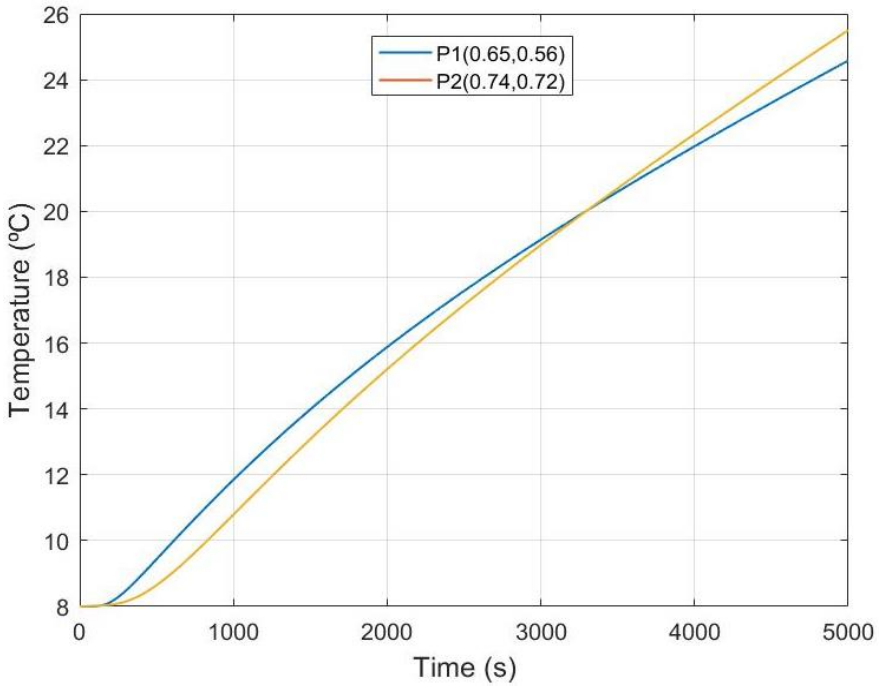

Figure 12: Comparison between the two requested points at 5000 seconds.

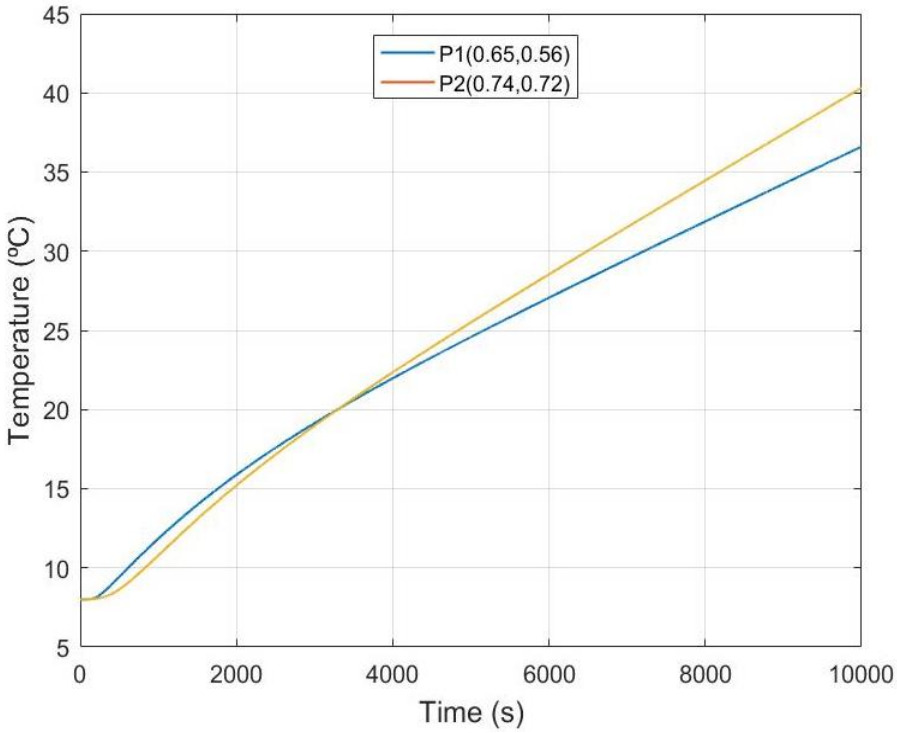

Figure 13: Comparison between the two requested points at 10000 seconds.

Tempo seconds	P1	P2		Tempo seconds	P1	P2
0.00	8.00	8.00		5000.00	24.58	25.50
20.00	8.00	8.00		5200.00	25.09	26.12
40.00	8.00	8.01		5400.00	25.59	26.73
80.00	8.00	8.01		5600.00	26.08	27.34
100.00	8.01	8.02		5800.00	26.58	27.94
400.00	8.94	8.35		6000.00	27.07	28.54
800.00	10.91	9.86		6200.00	27.55	29.14
1200.00	12.73	11.72		6400.00	28.04	29.74
1400.00	13.58	12.63		6600.00	28.52	30.34
1600.00	14.38	13.52		6800.00	29.01	30.93
1800.00	15.15	14.38		7000.00	29.49	31.52
2000.00	15.88	15.21		7200.00	29.97	32.11
2200.00	16.58	16.01		7400.00	30.45	32.70
2400.00	17.25	16.78		7600.00	30.93	33.29
2600.00	17.90	17.53		7800.00	31.40	33.88
2800.00	18.53	18.27		8000.00	31.88	34.47
3000.00	19.14	18.98		8200.00	32.35	35.06
3200.00	19.73	19.68		8400.00	32.83	35.65
3400.00	20.31	20.36		8600.00	33.30	36.23
3600.00	20.88	21.04		8800.00	33.78	36.82
3800.00	21.43	21.70		9000.00	34.25	37.40
4000.00	21.98	22.35		9200.00	34.72	37.99
4220.00	22.56	23.06		9400.00	35.20	38.57
4400.00	23.04	23.63		9600.00	35.67	39.16
4600.00	23.56	24.26		9800.00	36.14	39.74
4800.00	24.07	24.88		9999.00	36.61	40.32

Table 7: Temperatures values from 0 seconds to 10.000 seconds

4.3 The Diagonal Flow Problem

The flow is in the upper diagonal, and the boundary conditions are those that are shown in the image, the solution of this problem is known for an infinite Peclet number.

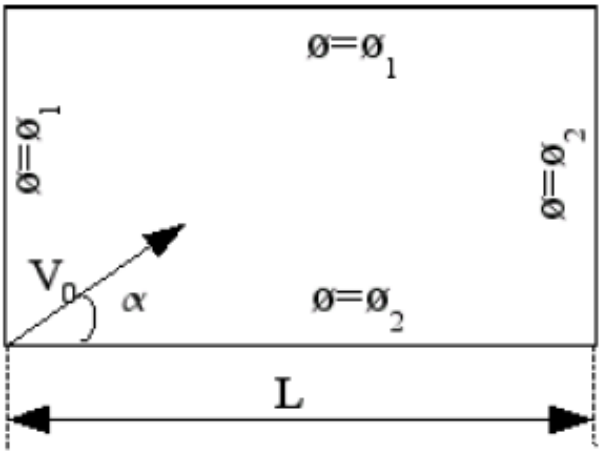

Figure 14: The Diagonal Flow Problem [10].

The velocity field in this case is as follows:

$$u(x,y) = V_0 \cdot cos(\alpha) \quad (4.23)$$
$$v(x,y) = V_0 \cdot sin(\alpha) \quad (4.24)$$

The solution must fulfil the following criteria:

$$\phi = \phi_1 \quad \text{Above the diagonal} \quad (4.25)$$
$$\phi = \phi_2 \quad \text{Below the diagonal} \quad (4.26)$$

To solve the problem two schemes were used the Upwind and Quick in order to compare a first order scheme with a second order scheme. On the other hand, the solver used for this case is a Line by Line method.

The results are divided in three sections;

- Rho/gamma = 10
- Rho/gamma = 1e3
- Rho/gamma = 1e6

Once the simulated results have been verified it is time to plot those results and thereafter analyze its behavior depending on the value of ρ/Γ.

Results

The results obtained with the created program are shown below. we have chosen two types of mesh disinfection, 50 x 50 and 100 x 100. The Peclet number will be varied to see the behavior with different numbers. For the different cases a comparison by means of graphs of the two schemes were adopted. We can observe that the results are similar in the two schemes and we also see a better result that approaches the theoretical by applying meshes with more numbers of nodes.

1. **Rho/gamma = 10**

a) UpWind

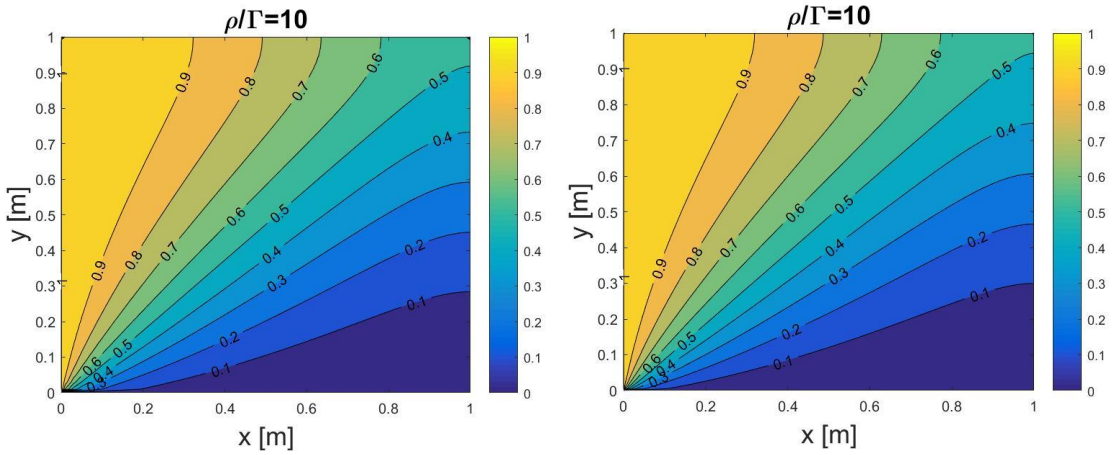

Figure 15: Mesh Comparison 50 x 50 and 100 x 100.

b) Quick

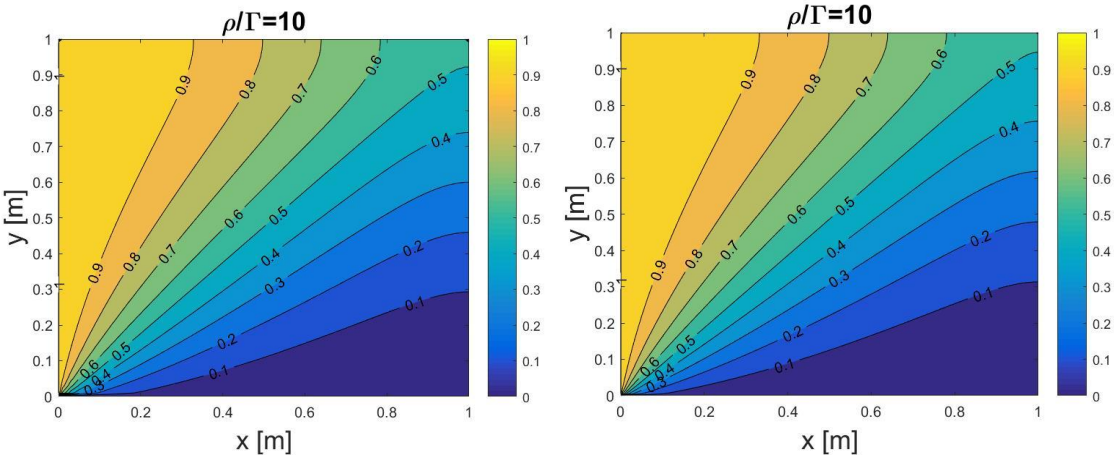

Figure 16: Mesh Comparison 50 x 50 and 100 x 100.

2. Rho/gamma = 1000

The results obtained for the simulation are presented for a Re = 1e3, with a mesh of 50 x 50 and 100 x 100 with an error 1e-6.

a) UpWind

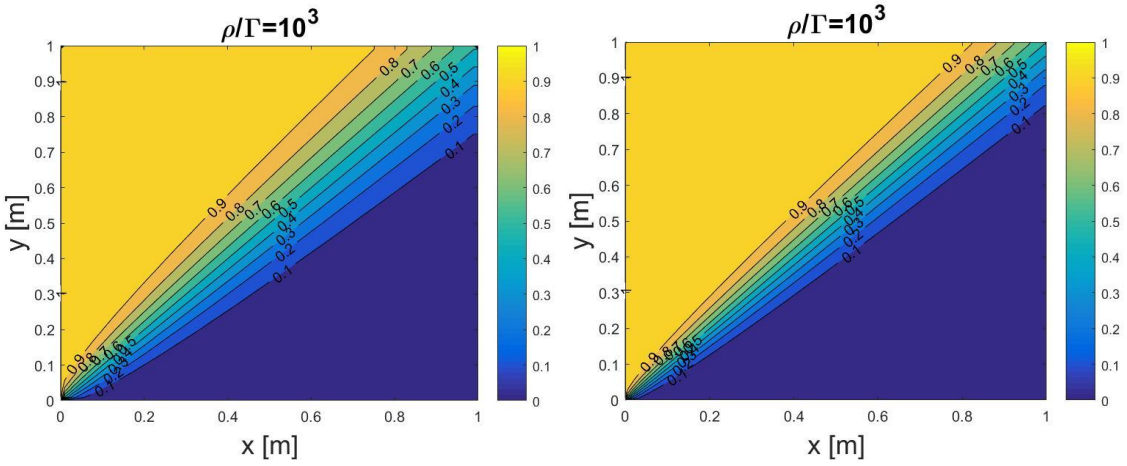

Figure 17: Mesh Comparison 50 x 50 and 100 x 100.

b) Quick

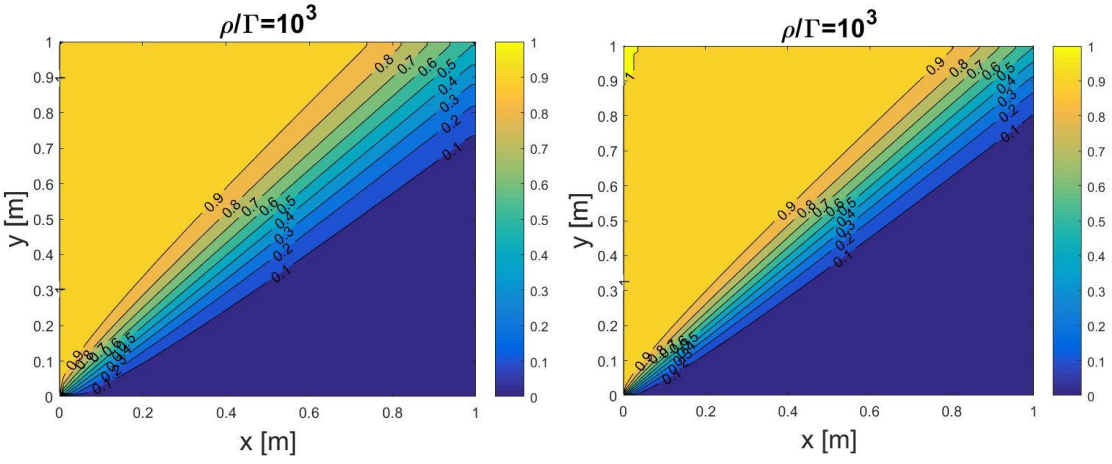

Figure 18: Mesh Comparison 50 x 50 and 100 x 100.

3. Rho/gamma = 1000000

The results obtained for the simulation are presented for a Re = 1e6, with a mesh of 50 x 50 and 100 x 100 with an error 1e-6.

a) Upwind

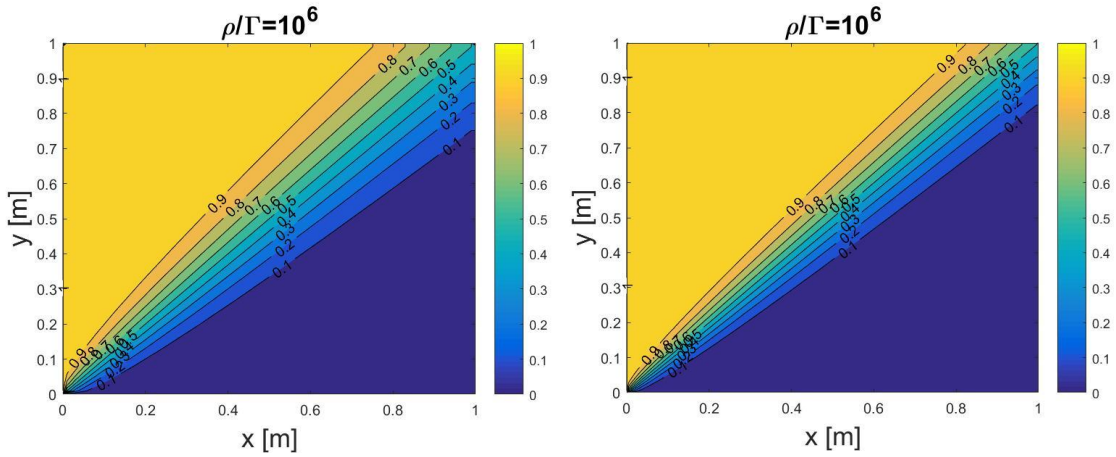

Figure 19: Mesh Comparison 50 x 50 and 100 x 100.

b) Quick

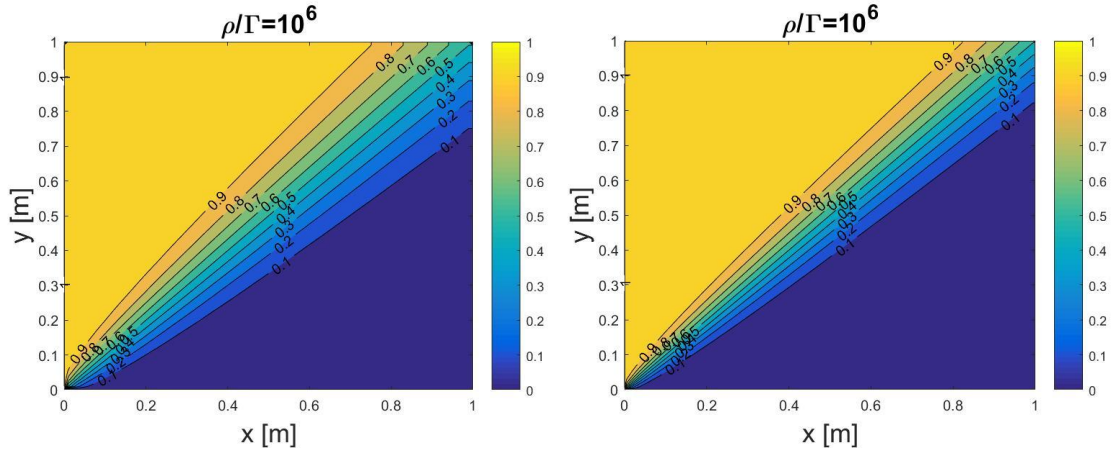

Figure 20: Mesh Comparison 50 x 50 and 100 x 100.

As can be seen in the cases studied, the problems are very sensitive to Peclet variations. For low values, a large diffusion zone is obtained where the variable does not have the expected value, and as the number of Péclet increases, this diffusion is reduced, and the result approaches the theoretical one. However, the exercise is also sensitive to the meshing used, as can be seen in the previous figures. For less dense meshes the phenomenon known as false diffusion occurs, where it seems that there is more diffusion than there really is, as if the value of the simulated Péclet was lower than the real one, while for denser meshes, diffusion is reduced, and the value obtained is closer to the ideal.

4.4 The Smith Hutton Problem

The objective of the problem is to solve the transport of a variable due to a constant velocity field into a bi-dimensional body testing different numerical schemes.

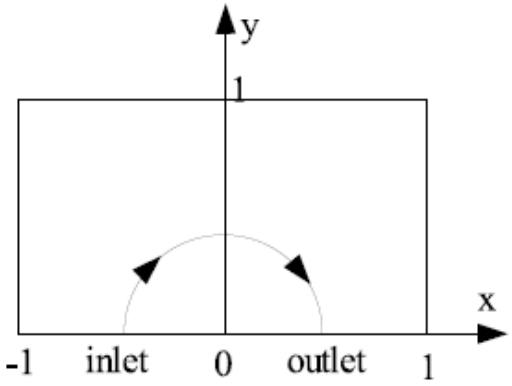

Figure 21: The Smith Hutton Problem[9].

This problem is also known as the Smith-Hutton problem and has the peculiarity that the flow moves solenoidal, so that for a rectangular domain like the one observed in the image, the velocity field is of the form:

$$u(x,y) = 2y(1-x^2) \quad (4.27)$$

$$v(x,y) = -2x(1-y^2) \quad (4.28)$$

And the boundary conditions of the study variable are those shown in the table below, where the value of α must be 10 for this exercise:

Boundary Conditions		
ϕ = 1+ tanh [(2x +1) α]	-1 < x < 0	y = 0 (entrance)
ϕ = 1- tanh [α]	x = -1	0 < y < 1
ϕ = 1- tanh [α]	-1 < x < 1	y = 1
ϕ = 1- tanh [α]	x = 1	0 < y < 1
$\frac{\partial \phi}{\partial y} = 0$	0 < x <1	y = 0 (exit)

Table 8: Phi value related to the Boundary Conditions.

For the development of this problem we will assume different hypotheses that will help us to build the program. One of the first hypotheses is that the flow is steady state, thermophysical parameters such as density and diffusion coefficient are constant and cell-centered discretization: average values over each cell –the property ϕ, density, diffusion coefficient.

Matematical Formulation of the Problem

In order to solve this case, the convection-diffusion equation has to be solved.

$$\frac{\partial \rho \phi}{\partial t} + \nabla \cdot (\rho \vec{v} \phi) = \nabla \cdot (\Gamma \nabla \phi) + S \tag{4.29}$$

To discretize the convection-diffusion equation, it has been used the Finite Volume Method (FVM) as shown in the equation below.

$$\left(\frac{\partial \rho \phi}{\partial t}\right)_p \Delta x \Delta y + ((\dot{m}\phi)_e - (\dot{m}\phi)_w)\Delta y + (\dot{m}\phi)_n - (\dot{m}\phi)_s)\Delta x = \left(\Gamma \frac{\partial \phi}{\partial x} S\right)_e - \left(\Gamma \frac{\partial \phi}{\partial x} S\right)_w + \left(\Gamma \frac{\partial \phi}{\partial x} S\right)_n - \left(\Gamma \frac{\partial \phi}{\partial x} S\right)_s \tag{4.30}$$

Results

The results obtained with UDS and Quick Scheme are shown in the following pages, these results are comparing with the reference results.

The results are divided in three sections;

- Rho/gamma = 10
- Rho/gamma = 1e3
- Rho/gamma = 1e6

Once the simulated results have been verified it is time to plot those results and thereafter analyze its behavior depending on the value of ρ/Γ. The results can vary according to the mesh number, so we can see that the density of the mesh is a very important factor when it comes to obtaining accurate results.

Finally, the results commented graphically will be seen. In the first case corresponding to $\rho / \Gamma =$ 10 and 300 x150 mesh, the diffusion present in the domain is higher than in the other two cases, due to the low convective term, while in the other two cases, for higher ρ / Γ values and a higher mesh density, diffusion is lower, and the strong effect of convection is seen, moving the fluid according to the geometry of the velocity field.

1. Rho/gamma = 10

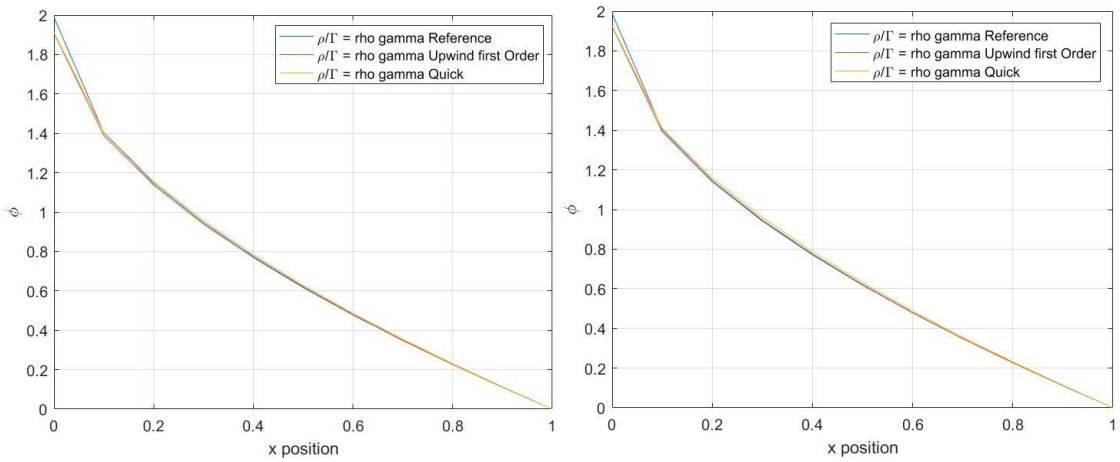

Figure 22: Mesh Comparison 200 x 100 and 300 x 150.

2. Rho/gamma = 1e3

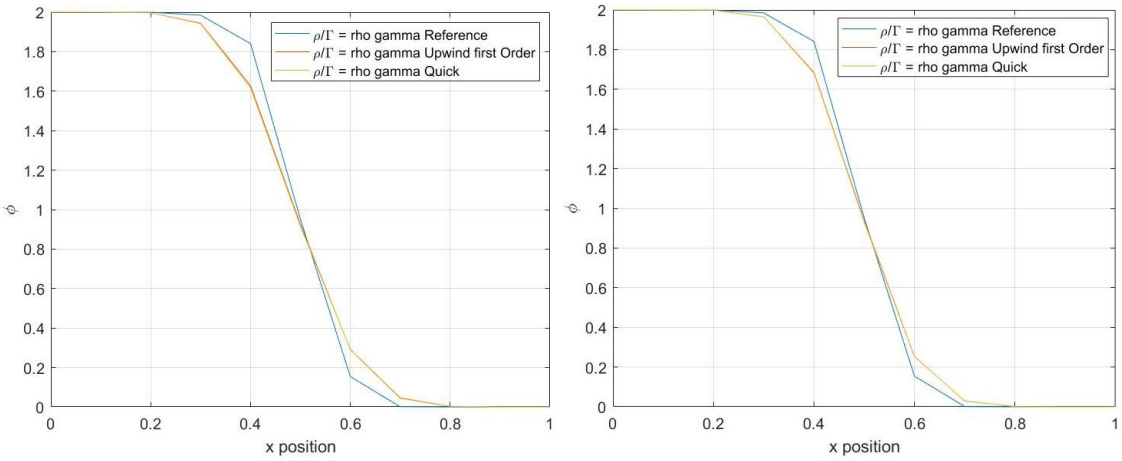

Figure 23:Mesh Comparison 200 x 100 and 300 x 150.

3. Rho/gamma = 1e6

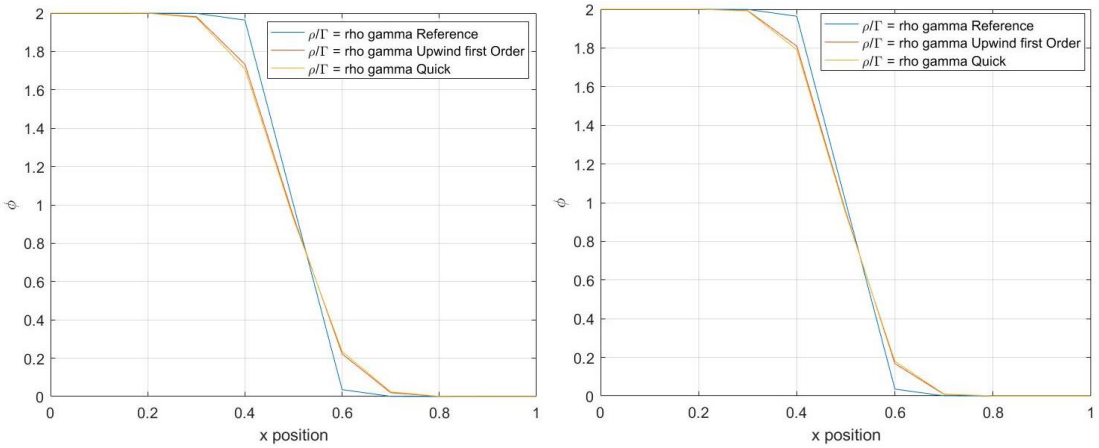

Figure 24: Mesh Comparison 200 x 100 and 300 x 150.

The following table contains the numerical values of the different numbers of ρ/Γ with the two schemes chosen for the comparison with the reference. The Mesh used to obtain the following values is a 200 x100.

	Rho/Gamma 10			Rho/Gamma 1000			Rho/Gamma 1000000		
Position x	Reference	QUICK	UDS	Reference	QUICK	UDS	Reference	QUICK	UDS
0.0	1.989	1.911	1.908	2.000	2.000	2.000	2.000	2.000	2.000
0.1	1.402	1.404	1.387	1.999	1.999	1.999	2.000	2.000	2.000
0.2	1.146	1.155	1.136	1.999	1.997	1.997	2.000	1.999	1.999
0.3	0.946	0.956	0.938	1.985	1.942	1.944	1.999	1.977	1.981
0.4	0.775	0.784	0.769	1.841	1.617	1.627	1.964	1.708	1.733
0.5	0.621	0.629	0.617	0.951	0.916	0.924	1.000	0.925	0.936
0.6	0.480	0.486	0.477	0.154	0.292	0.290	0.036	0.234	0.222
0.7	0.349	0.353	0.348	0.001	0.046	0.044	0.001	0.024	0.020
0.8	0.227	0.230	0.226	0.000	0.003	0.003	0.000	0.000	0.007
0.9	0.111	0.113	0.111	0.000	0.000	0.000	0.000	0.000	0.000
1.0	0.000	0.000	0.000	0.000	0.000	0.000	0.000	0.000	0.000

Table 9: Different rho/gamma comparison

Below the plots of the results obtained for the different numbers of ρ/Γ, in which the diffusion that originates when the value of x is low can be better appreciated.

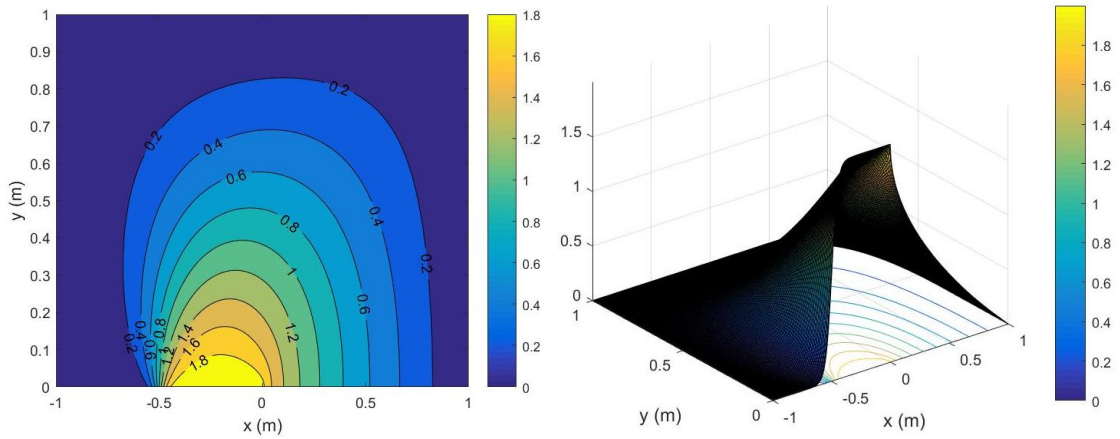

Figure 25: 2D plots with Rho/Gamma 10

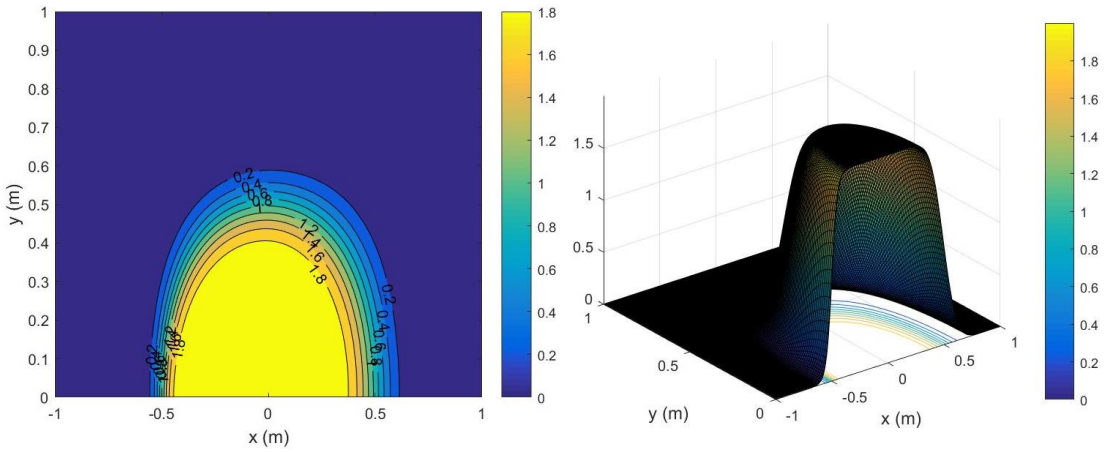

Figure 26:2D plots with Rho/Gamma 1000

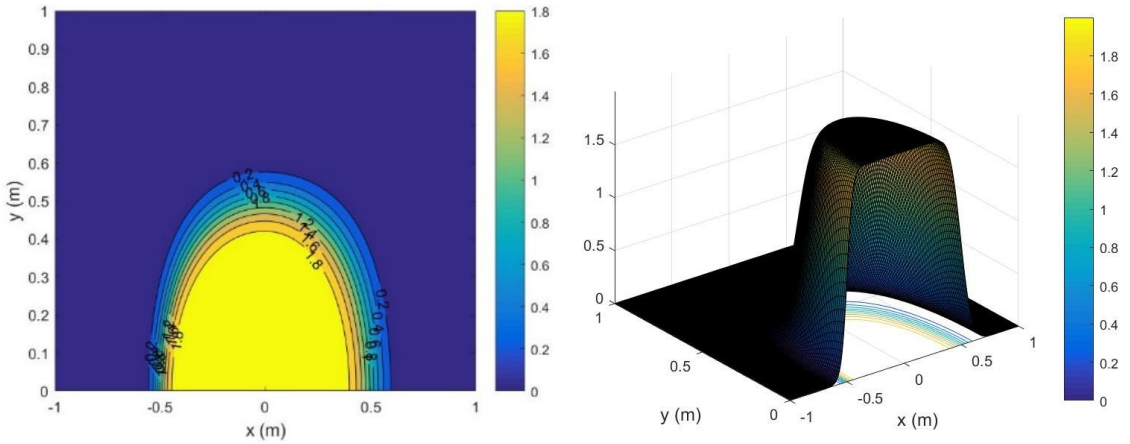

Figure 27: 2D plots with Rho/Gamma 1000000

The two schemes used are almost similar, the Quick is the one that comes closest to the reference. So, the Quick scheme is much more accurate than the UDS.

Looking of the simulated figures, it can be appreciated how in the first case the velocity enters in the cavity and by diffusion is dispersed through the cavity. But, in the other cases, where the Peclet has been increased, the diffusive term does not affect so much, and the velocity enters in the cavity and goes off by convection. In conclusion, if the Peclet increases the convective term is the dominants over the diffusive one, or vice versa if the Peclet number decreases.

4.5 Summary chapter

During this chapter we have seen how to implement the Navier-Stokes equations in their incompressible form for the 3 case studies.

In the first case we have discretized the convection-diffusion equations for the case under examination, we have applied certain hypotheses that allow us to solve the problem more easily. For the temporary discretization, an implicit method has been chosen and for the spatial discretization the FVM as well as for the other two study cases. The boundary conditions imposed by the problem have been followed resulting in a great similarity with the theoretical data. Table 7 shows how the two points assigned by the problem vary each time the time advances, this variation can be better appreciated in figure 12 and 13.

For Diagonal Flow as can be seen, the problems are very sensitive to Peclet variations. For low values, a large diffusion zone is obtained where the variable does not have the expected value, and as the number of Péclet increases, this diffusion is reduced, and the result approaches the theoretical one. However, the exercise is also sensitive to the meshing used, as can be seen in the previous figures. For less dense meshes the phenomenon known as false diffusion occurs, where it seems that there is more diffusion than there really is, as if the value of the simulated Péclet was lower than the real one, while for denser meshes, diffusion is reduced, and the value obtained is closer to the ideal.

And finally, for the Smith-Hutton problem, it can be appreciated how in the first case (Re = 10) the velocity enters in the cavity and by diffusion is dispersed through the cavity. But, in the other cases, where the Peclet has been increased, the diffusive term does not affect so much, and the velocity enters in the cavity and goes off by convection. In conclusion, if the Peclet increases the convective term is the dominants over the diffusive one, or vice versa if the Peclet number decreases.

The codes made in Matlab have responded to the physics of the problems under study therefore we can say that the problems set at the beginning of the chapter have been solved.

5. Fraction Step Method

5.1 Introduction

The set of Navier-Stokes equations and the continuity equation make up a complex system of differential equations in coupled partial derivatives. That is why, except for very simple cases, no analytical solutions have yet been found and the need for a numerical resolution is evident.

The process of obtaining the numerical solution computationally involves three stages, decoupling, discretizing and solving the equations. In the first stage, we try to decouple the speed of the pressure in the equations, it means, to find an adequate method that allows us to obtain a set of equivalent expressions to the Navier-Stokes equations and continuity, in which the unknowns ($\vec{v}\ and\ p$) can be solved separately. In the second stage, the differential equations in partial derivatives and their boundary conditions are transformed into a system of discrete algebraic equations, both in time and space. Finally, the third stage involves the implementation of numerical methods to computationally solve systems of algebraic equations already discretized and decoupled.

In this chapter we will study, on the one hand, the so-called fractional steps method (Fractional-Step Method-FSM), a method used to decouple the velocity pressure in the Navier-Stokes equations, and on the other hand, the Finite Volumes method, used to spatially discretize the equations. During the development of the FSM, the discretization schemes used for the temporary part will also be explained.

5.2 FSM

This method uses the decomposition theorem of Helmholtz-Hodge to solve the coupling of pressure and velocity in incompressible fluids. The idea is to obtain two separate equations, one for speed and one for pressure. For this the method uses an intermediate speed with which the pressure is resolved and then the final speed is calculated by correcting the intermediate speed with the pressure. Below we will see in more detail the operation of the method, starting with the Helmholtz-Hodge theorem[11].

The Helmholtz-Hodge theorem states that any vector field in a closed contour can be uniquely decomposed into a part of zero divergence or solenoidal part and an irrotational part, as follows:

$$\vec{\omega} = \vec{\omega}_{sol} + \vec{\omega}_{irr} = \vec{\omega}_{sol} + \vec{\nabla}A \tag{5.1}$$

The figure below shows the decomposition of the vector field $\vec{\omega}$

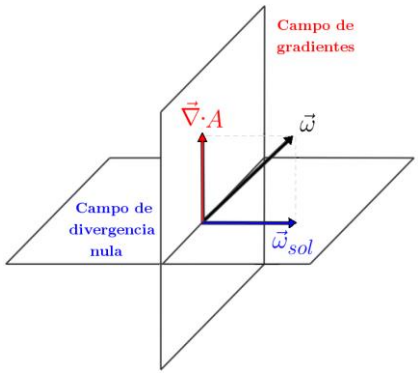

Figure 28: Decomposition of the vector field $\vec{\omega}$.

Obtaining $\vec{\nabla}A \; x \; \vec{\nabla}A \; = \; 0$ to any scalar field A. Applying the divergence operator on both sides of equation (5.1) ($\vec{\nabla} \cdot \; \vec{\omega}_{sol} = \; 0$) the Poisson equation for the scalar field A is obtained.

$$\vec{\nabla} \cdot \; \vec{\omega} \; = \; \nabla^2 \; A \tag{5.2}$$

If the field is known, the above equation can be solved using the following relationship:

$$\vec{\omega}_{sol} \; = \; \vec{\omega} \; - \; \vec{\nabla}A \tag{5.3}$$

Once explained the Helmholtz-Hodge theorem we apply it to the Navier-Stokes equations to solve the coupling of pressure and velocity and obtain two resolvable equations, one for each variable mentioned.

$$\frac{\partial \vec{v}}{\partial t} \; + \; \left(\vec{v} \; \cdot \; \vec{\nabla}\right)\vec{v} \; = \; \frac{1}{Re} \; \nabla^2 \vec{v} \; - \; \vec{\nabla}p \tag{5.4}$$

$$\vec{\nabla} \; \cdot \; \vec{v} \; = \; 0 \tag{5.5}$$

The term of the pressure corresponds with the irrotational part that we mentioned ($\vec{\nabla}p \sim \vec{\nabla}A$), and the velocity with the field of divergence null $\vec{\nabla} \; \cdot \; \vec{v} \sim \vec{\nabla} \cdot \; \vec{\omega}_{sol}$. Therefore, the method consists in defining an intermediate speed that corresponds to the solenoidal field and that is a function of a vector that we will define as R ($\vec{v}$). Then, if we separate the term of the pressure in (5.4) and apply the divergence operator, we obtain the Poisson equation for the pressure.

$$\nabla^2 p = \vec{\nabla} \cdot \left[-(\vec{v} \cdot \vec{\nabla})\vec{v} + \frac{1}{Re} \nabla^2 \vec{v} \right] \tag{5.6}$$

$$\mathrm{R}(\vec{v}) = \left[-(\vec{v} \cdot \vec{\nabla})\vec{v} + \frac{1}{Re} \nabla^2 \vec{v} \right] \tag{5.7}$$

Using $\mathrm{R}(\vec{v})$, an analogous equation as (5.3) is obtained for the Navier-Stokes equations (see figure):

$$\vec{v} = \mathrm{R}(\vec{v}) - \vec{\nabla} p$$

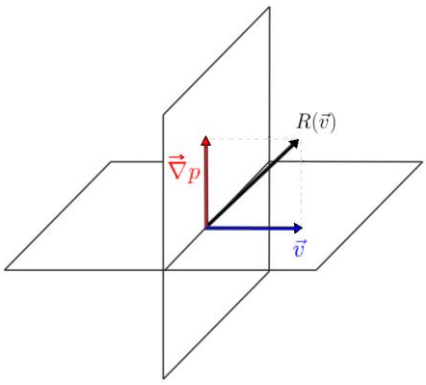

Figure 29: Decomposition of the Navier-Stokes equations in an irrotational field irrotational and one of null divergence.

In this way, with the initial velocity field (which is known), we can directly calculate the intermediate velocity $\vec{v} * = f\left(R(\vec{v})\right)$, use it to solve the Poisson equation, and finally correct $\vec{v} *$ with the pressure gradient to calculate the final velocity $\vec{v}$ fluid.

Temporal discretization

Explicit schemes will be used to reduce computational time, and to solve the stability problem, the Courant criterion will be used to determine the time step:

$$C_0 = \frac{|u|\Delta t}{\Delta x} \leq 1 \tag{5.8}$$

Following now with the choice of the temporal schemes for the development of the FSM, in our case we have opted for a low order scheme CDS (Central Difference Scheme) for the discretization of the term of the temporary derivative,

$$\left.\frac{\partial \vec{v}}{\partial t}\right|_{n+1/2} \approx \frac{\vec{v}^{n+1} - \vec{v}^{n}}{\Delta t} \tag{5.9}$$

an explicit scheme of the second order known as the Adams-Bashforth scheme for the terms grouped in $R(\vec{v})$,

$$R^{n+1/2}(\vec{v}) \approx \frac{3}{2}R(\vec{v}^{n}) - \frac{1}{2}R(\vec{v}^{n-1}) \tag{5.10}$$

and finally, a Euler backward first order scheme for the term of the pressure gradient:

$$\frac{\vec{v}^{n+1} - \vec{v}^{n}}{\Delta t} = \frac{3}{2}R(\vec{v}^{n}) - \frac{1}{2}R(\vec{v}^{n-1}) - \vec{\nabla}p^{n+1} \tag{5.11}$$

Now, reorganizing the equation (5.11), the intermediate velocity is obtained, represented by the first term of the following expression:

$$\vec{v}^{n+1} + \vec{\nabla}p^{n+1}\Delta t = \vec{v}^{n} + \Delta t\left[\frac{3}{2}R(\vec{v}^{n}) - \frac{1}{2}R(\vec{v}^{n-1})\right] \tag{5.12}$$

$$\vec{v}* = \vec{v}^{n+1} + \vec{\nabla}p^{n+1}\,\Delta t \tag{5.13}$$

In this way an expression is obtained to determine the real speed $\vec{v}^{n+1}$. The last step is to apply to the equation (5.13) the divergence operator and the incompressibility criterion to obtain the Poisson equation in a discrete form, thus concluding with the formulation of the method.

$$\vec{\nabla}\,\vec{v}* = \Delta t\,\nabla^2\,p^{n+1}$$

FSM Steps

The resolution steps of the FSM will be summarized below. In this way we will see both the global operation that the program will follow and the equations with which we will work from now on to complete the process of discretization.

1. Evaluating the diffusive and convective terms by calculating $R(\vec{v}^n)$ using the initial velocity field.

$$R(\vec{v}^n) = -(\vec{v}^n \Delta t)(\vec{v}^n) + \frac{1}{Re} \nabla^2 \vec{v}^n \tag{5.14}$$

2. Determine the intermediate speed

$$\vec{v}* = \vec{v} + \Delta t \left[\frac{3}{2} R(\vec{v}^n) - \frac{1}{2} R(\vec{v}^{n-1}) \right] \tag{5.15}$$

3. Solve the Poisson equation to obtain the pressure fields.

$$\nabla^2 p^{n+1} = \frac{\vec{\nabla} \cdot \vec{v}*}{\Delta t} \tag{5.16}$$

4. Correct the intermediate speed with the pressure of the previous step and evaluate the actual velocity of the fluid at the instant n+1

$$\vec{v}^{n+1} = \vec{v}* - \vec{\nabla} p^{n+1} \Delta t \tag{5.18}$$

5.3 Spatial Discretization

5.3.1 Finite Volume Method

The method of finite volumes is based on the direct discretization of the equations of conservation of the mass, motion and energy. This method integrates the equations in each of the control volumes in which the work domain is divided (see Figure 30), associating each of them with a nodal point in the center. The surface integrals that appear in the equations are approximated by the sum of the flows that cross each of the faces of the polyhedron; the result is a discretized equation that relates the values of the variables in a group of nodal points[8].

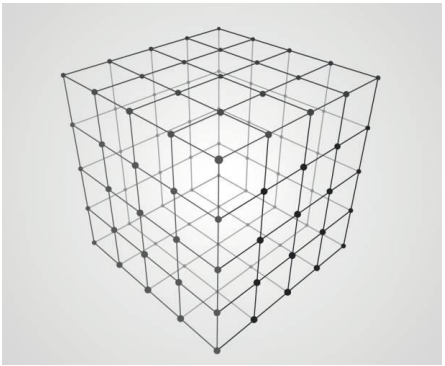

Figure 30: The finite volume Method

The main advantage of this method is that spatial discretization is carried out directly in the physical space of the problem. Therefore, there are no problems with the transformation between coordinate systems, as in the finite differences method. Another advantage of the method is the great flexibility it offers when using it in both structured and unstructured meshes. Due to all this this method is one of the most used in CFD simulations.

5.3.2 Grid

The first step in spatial discretization consists of the discretization of the work domain, that is, deciding the most appropriate type of mesh to our problem, considering the advantages and limitations of each of them.

Depending on the shape and relative size of the nodes that make up a mesh, two types are distinguished, the structured and unstructured meshes. Within the structured meshes we can find uniform or non-uniform meshes, depending on the regularity of the spacing between cells.

The advantage of structured meshes is that their geometry is simple and therefore are easier and intuitive to program. However, they are not perfectly adaptable to the regions of interest and it is not possible to densify an area of interest without increasing the number of points along the entire mesh. The strong point of the unstructured meshes is precisely that they are totally moldable according to the geometry of the problem, but its implementation in the computer is quite more expensive. Therefore, it is necessary to define and decide what type of mesh is more convenient, considering the limitations of each one. For this case it will only be treated with simple geometries and therefore uniform structured meshes will be used. On the other hand, if we look at the situation of the nodes in the meshes, two types are distinguished: the centered meshes and the displaced meshes (staggered).

The centered ones are characterized by working with all the variables defined in the central node of the control volume, while the displaced meshes work with the pressure in the center of the volume and the components of the velocity are moved half a cell towards the face of the same.

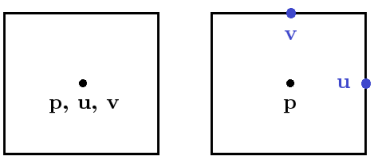

Figure 31: Example of centered mesh (left) and displaced mesh (right).

Working with a displaced mesh is equivalent to working with several centered meshes, one for each variable, as shown in Figure 32.

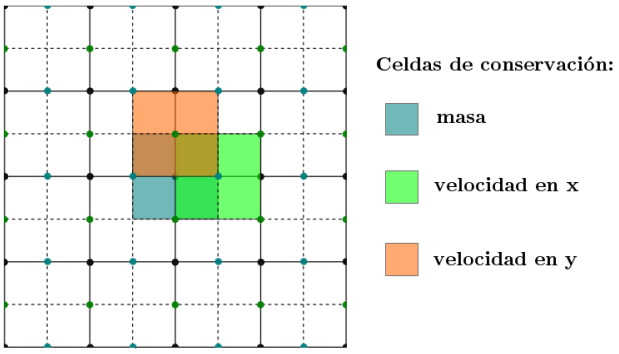

Figure 32: Example of displaced mesh in 2D.

The use of a displaced arrangement [12] such as that shown in Figure 31 has the advantage that many of the terms that require interpolation with the centered mesh can be calculated directly without interpolation. We can see this in figure 33. Both the pressure and the diffusive terms can be approximated by centered differences without interpolation, since the pressure is in the center of the cell and the velocity derivatives (needed for the term diffusive), are already calculated on the faces.

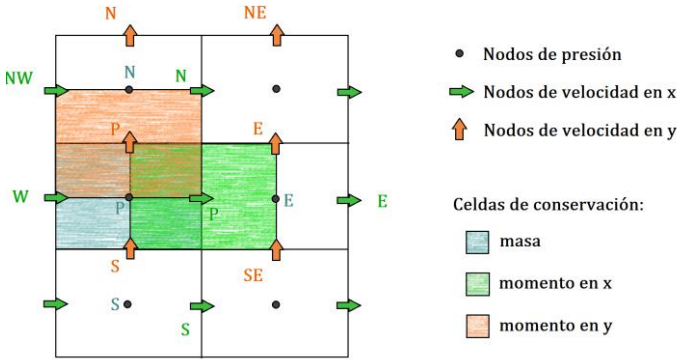

Figure 33: Representative diagram of the mesh used (uniform, structured and dispaced), as well as the placement of each of the points of the different variables.

Considering all the above, we will work with a uniform structured and displaced mesh. Figure 33 shows a scheme of the mesh that has been implemented, as well as the notation used of the cells and their adjoining ones. Given any point P, its neighbors will be denoted by the initials in English of the cardinal points, N, S, E and W. The faces of the cells are denoted in the same way but with lowercase letters.

5.3.3 Spatial Discretization of the Equations

The next step is to discretize the equations obtained in the "Steps of the FSM " section, thus eliminating the spatial derivatives involved. For this, the Finite Volumes method will be applied, so that the equations will be integrated over a generic cell like the one shown in figure 34, validating whether one component or another of the velocity is integrated. Initially, all the equations referring to one component and then the other should be integrated, each one integrated in its corresponding working mesh (Figure 33). However, the process can be simplified by integrating the equations for a generic variable $\phi = \vec{v} = (u, v)$ specifying which magnitudes have to be replaced or obtained from each particular mesh.

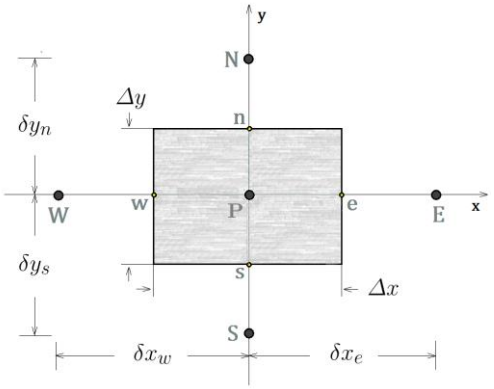

Figure 34: Generic cell diagram and nomenclature used to designate the parameters of the same.

The following equations will be discretized

$$\mathrm{R}(\phi) = -\left(\phi\,\vec{\nabla}\right)\phi + \frac{1}{Re}\,\nabla^2\,\phi \tag{5.19}$$

$$\nabla^2 p = \frac{\vec{\nabla}\cdot\vec{\phi}\,*}{\Delta t} \tag{5.20}$$

Then the discretization process will be shown for R (ϕ) Because the operators involved in the two equations are the same and the discretization is equivalent. The only difference, as we have mentioned before, is the work mesh, which for the equation (5.20) would be the mesh of the pressure nodes.

R (ϕ) Discretization

A. Convective term $\mathrm{R}(\phi)_{conv} = \left(\left(\phi\,\vec{\nabla}\right)\phi\right)$:

$$\iint_S R(\phi)_{conv}\,dS = \int_s^n \int_w^e \left(u\frac{\partial\phi}{\partial x} + v\frac{\partial\phi}{\partial y}\right)dx\,dy \tag{5.21}$$

$$\int_s^n \left[(u\,\phi)_e - (u\,\phi)_w + v\frac{\partial \phi}{\partial y}(x_e - x_w)\right] dy \tag{5.22}$$

$$[(u\,\phi)_e - (u\,\phi)_w](y_n - y_s) + [(v\,\phi)_n - (v\,\phi)_s]\,\Delta x \tag{5.23}$$

In the previous expression, we have approximated the surface integrals by the sum of the flows that cross the faces, $\phi_i = \phi_{e,w,n,s}$. Now, the points *e*,*w*,*n* and *s* are not points belonging to the working domain of the mesh and you need to put them in function of the points *E*,*W*,*N* and *S*. Using again the scheme of centered differences we can approximate:

$$\phi_i = \frac{\phi_P + \phi_I}{2} \tag{5.24}$$

Where $\phi_P and\ \phi_I = \phi_{E,W,N,S}$, Now theses flow corresponds to the mesh points. Substituting in equation (5.24) the following equation is obtained.

$$R\,(\phi)_{conv} = \frac{\Delta y}{2}[u_e(\phi_P + \phi_E) - u_w(\phi_P + \phi_W)] + \frac{\Delta x}{2}[v_e(\phi_P + \phi_E) - v_w(\phi_P + \phi_S)] \tag{5.25}$$

B. Diffusive part $R\,(\phi)_{dif} = \nabla^2\phi$:

$$\iint_S \nabla^2\phi\ dS = \int_s^n \int_w^e \left(\frac{\partial^2\phi}{\partial x^2} + \frac{\partial^2\phi}{\partial y^2}\right) dx\,dy \int_s^n \left[\left(\frac{\partial\phi}{\partial x}\right)_e - \left(\frac{\partial\phi}{\partial y}\right)_w + \frac{\partial^2\phi}{\partial y^2\Delta}\Delta x\right] dy = \Delta y\left[\left(\frac{\partial\phi}{\partial x}\right)_e - \left(\frac{\partial\phi}{\partial x}\right)_w\right] + \Delta x\left[\left(\frac{\partial\phi}{\partial y}\right)_n - \left(\frac{\partial\phi}{\partial y}\right)_s\right] \tag{5.26}$$

This time to obtain the expression based on the points of the domain again centered differences will be used in the following way:

$$\left(\frac{\partial\phi}{\partial x}\right)_i = \frac{\phi_I - \phi_P}{x_I - x_P} \qquad \left(\frac{\partial\phi}{\partial y}\right)_i = \frac{\phi_I - \phi_P}{y_I - y_P} \tag{5.27}$$

Substituting in the equation (5.27), the following expression for the diffusive part is obtained

$$R(\phi)_{dif} = \Delta y\left[\left(\frac{\phi_E - \phi_P}{\delta x_e}\right) - \left(\frac{\phi_E - \phi_W}{\delta x_w}\right)\right] + \Delta x\left[\left(\frac{\phi_N - \phi_P}{\delta y_e}\right) - \left(\frac{\phi_P - \phi_S}{\delta y_w}\right)\right] \quad (5.28)$$

The next step is to add the convective and the diffusive terms considering that $-R(\phi)_{conv} + \frac{1}{Re} R(\phi)_{dif}$. the following expression is obtained:

$$R(\phi) = \frac{\Delta y}{2}[u_w(\phi_P + \phi_W) - u_e(\phi_P + \phi_E)] + \frac{\Delta x}{2}[v_s(\phi_P + \phi_S) - v_n(\phi_P + \phi_N)] + \frac{1}{Re}\Delta y\left[\left(\frac{\phi_E - \phi_P}{\delta x_e}\right) - \left(\frac{\phi_P - \phi_W}{\delta x_w}\right)\right] + \frac{1}{Re}\Delta x\left[\left(\frac{\phi_N - \phi_P}{\delta y_n}\right) - \left(\frac{\phi_P - \phi_S}{\delta y_s}\right)\right] \quad (5.29)$$

The above equations can be expressed in the following form;

$$R(\phi) = a_W\phi_W + a_E\phi_E + a_N\phi_N + a_S\phi_S - a_P\phi_P \quad (5.30)$$

West nodes

$$a_W = \Delta y\left(\frac{1}{Re\ \delta x_w} + \frac{u_w}{2}\right) \quad (5.31)$$

East nodes

$$a_E = \Delta y\left(\frac{1}{Re\ \delta x_e} + \frac{u_e}{2}\right) \quad (5.32)$$

North nodes

$$a_N = \Delta x\left(\frac{1}{Re\ \delta y_n} + \frac{v_n}{2}\right) \quad (5.33)$$

South nodes

$$a_S = \Delta x\left(\frac{1}{Re\ \delta y_s} + \frac{v_w}{2}\right) \quad (5.34)$$

$$a_P = a_W + a_E + a_N + a_S \quad (5.35)$$

5.4 Algorithm

1. *Case Definition*

The definition of the case is an essential part of the whole process. At this point, the chosen physical problem is transformed into a set of discretized equations and the appropriate boundary conditions are established. Likewise, we opt for a specific spatial and temporal discretization, and finally the criteria for convergence of the program are chosen.

2. *Pre-Processing*

In this second phase of the process, once the choice of the case has been stipulated, on the one hand the physical data and numerical parameters related to it are introduced, and on the other hand, the necessary calculations are made prior to the iterative body. In this way, the main steps of this phase will be the following:

- Introduce the geometric parameters necessary for the creation of the mesh.
- Introduce the physical parameters, which depend on the choice of the case, although in a general way they could be the viscosity, density, initial speed, Reynolds number etc.
- Introduce the numerical integration parameters related to the convergence of the problem, that is, the desired precisions for the pressure and the components of the velocity.
- Finally, the matrix of pressure coefficients is calculated, and the empty matrices of the velocity components are defined.

3. *Iterative body*

The iterative body is the most important part of the algorithm. This part is repeated many times until the convergence criteria is reached. it consists of the following points:

- The vector *R (ϕ)* is calculated for each component of the velocity from the initial velocity field, obtaining the convective and diffusive terms.
- From the above terms the intermediate speed is determined.
- The Poisson equation is solved, and the pressure is determined
- The intermediate speed is corrected with the pressure gradient and the actual speed of the fluid in the next time step.
- Finally, convergence criteria are established to ensure that the program ends when the velocities and pressure do not change over time.

5.5 Driven Cavity

The Driven cavity problem consists of a closed cavity of infinite length, with a fluid in its interior and one of the walls moving at a constant speed, as shown in figure 20. The mass in this system is conserved, so there is no entry or exit of mass in the cavity. This case is perfectly compatible with the specifications previously made in the equations, so incompressible and Newtonian fluids will be used in laminar regime. The equations of the movement that we will solve, therefore, the following:

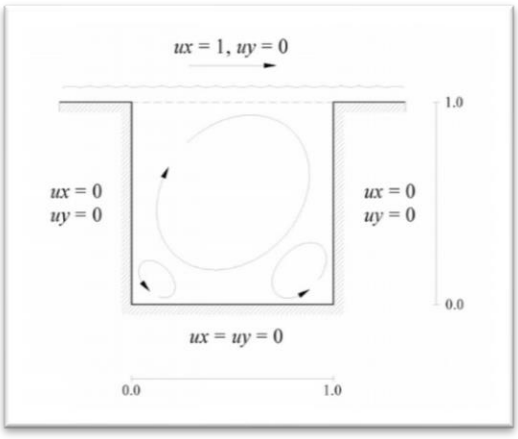

Figure 35: Outline of the geometry and boundary conditions of the Driven case

$$\frac{\partial U}{\partial x} + \frac{\partial V}{\partial y} = 0 \tag{5.36}$$

$$\frac{\partial U}{\partial t} + U\frac{\partial U}{\partial x} + V\frac{\partial U}{\partial y} = \frac{1}{Re}\left(\frac{\partial^2 U}{\partial x^2} + \frac{\partial^2 V}{\partial y^2}\right) - \frac{\partial p}{\partial x} \tag{5.37}$$

$$\frac{\partial V}{\partial t} + U\frac{\partial V}{\partial x} + V\frac{\partial V}{\partial y} = \frac{1}{Re}\left(\frac{\partial^2 U}{\partial x^2} + \frac{\partial^2 V}{\partial y^2}\right) - \frac{\partial p}{\partial y} \tag{5.38}$$

$$Re = \frac{U_0 l}{v} \tag{5.39}$$

l is the characteristic length, in this case the length of the cavity, l = 1 m.

Regarding the boundary conditions, as we can see in figure 35, there are three fixed walls and a fourth one moving at a constant speed, so the boundary conditions for the velocity in the fixed

walls will be of non-slip type, it means, all the components of the velocity equal to zero except for the U component in the mobile wall, which will have a Dirichlet type condition, that is, a known value U = 1 m = s. The boundary conditions for the pressure are Neumann type, which implies that the pressure derivative in the walls is null.

It is possible to predict in a qualitative way which is the physics that must obey the problem. As the wall (or lid) moves, it will begin to draw fluid until it meets the right wall of the box, which forces the fluid to descend. The same will happen with the other two remaining walls, so that a recirculation of the flow occurs, as seen in figure 35. On the other hand, near the wall a pressure gradient must be produced, so that a positive pressure in one of the corners moves the flow away from it, and a negative pressure in the other corner brings it closer.

5.6 Results

The results obtained with the program created for the problem driven cavity are shown below. On the one hand, a study of the influence of mesh densification will be carried out, and once the optimum mesh is chosen, a study of the problem based on the Reynolds number is made. As we have seen, the Reynolds number tells us how predominant the viscous forces in each fluid are, so by doing this analysis, we will see the behavior of the fluid in the cavity as a function of the viscosity. The Reynolds number will be varied from Re = 100 (higher viscosity) to Re = 2000 (lower viscosity), to always ensure the permanence of the fluid within the laminar regime. The simulation will be propagated starting from the fluid in the resting cavity until reaching the steady state, it means a state in which the fluid no longer varies explicitly with time. The convergence criterion that will be used to determine if the simulation is in the steady state is as follows:

$$\frac{\|U^{n+1}\| - \|U^{n}\|}{\|U^{n+1}\|} < k \tag{5.40}$$

$$\frac{\|V^{n+1}\| - \|V^{n}\|}{\|V^{n+1}\|} < k \tag{5.41}$$

So, it is being imposed that the relative error between each component of the speed in a moment of time and in the previous instant is less than k, an error that we consider adequate.

First a study of the number of cells in the mesh has been carried out to determine which mesh will be used from now on, using a Re = 100. When the number of cells is increased, the precision of the simulation should be higher, same way as computational time, so we must reach a compromise between both. Meshes of 10, 30 and 50 nodes were used in each direction.

Re = 10

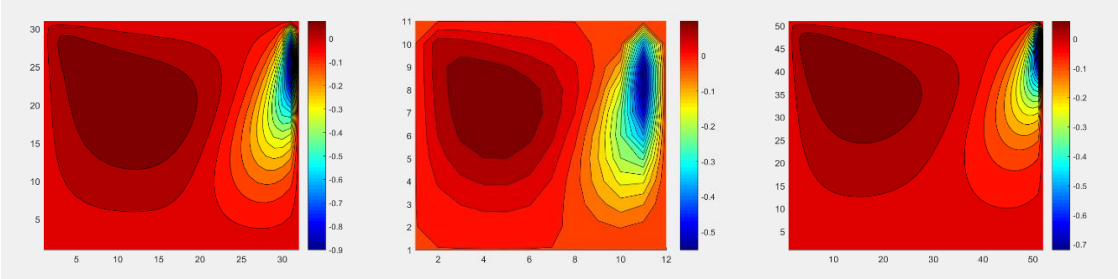

Figure 36: V (m/s), Mesh 10 x 10, 30 x 30, 50 x 50.

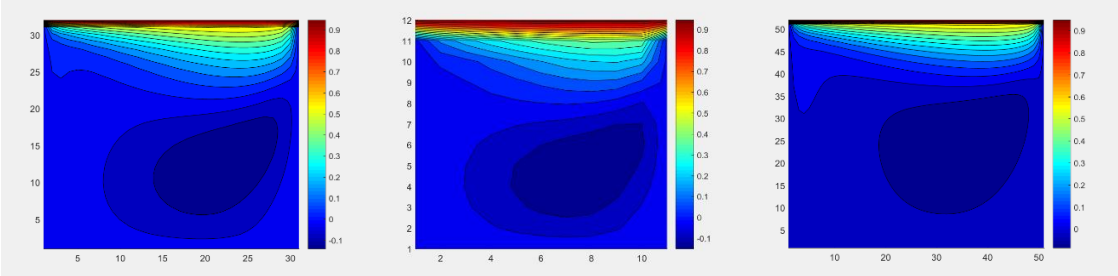

Figure 37: U (m/s), Mesh 10 x 10, 30 x 30, 50 x 50.

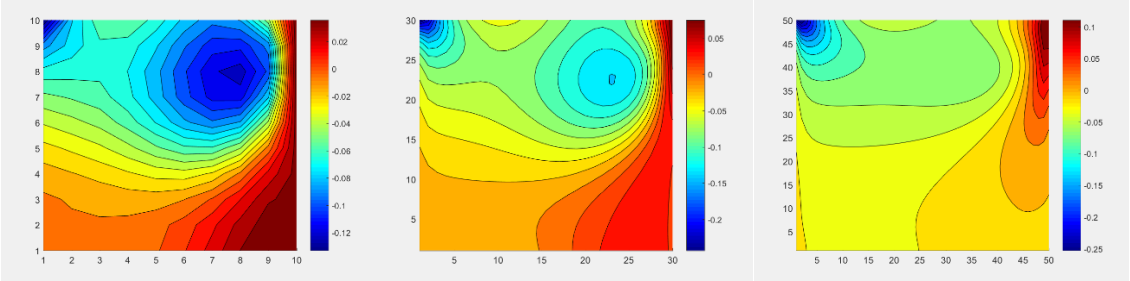

Figure 38: Pressure, Mesh 10 x 10, 30 x 30, 50 x 50.

In the previous figure we can visually compare the results obtained. However, sometimes a comparison by graphics is more effective, where solutions can be compared numerically. Therefore, the velocity profile of the component u will be shown below.

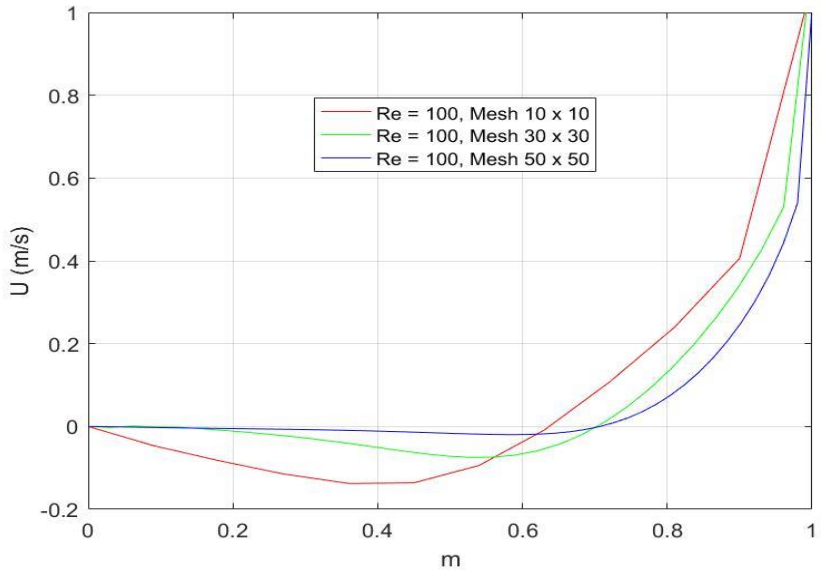

Figure 39: Mesh comparison U(m/s) with Re 100.

Re = 1000

The results obtained for the simulation are presented for a Re = 1000, with a mesh of 10 x 10, 30 x 30, 50 x 50 with an error 1e-6.

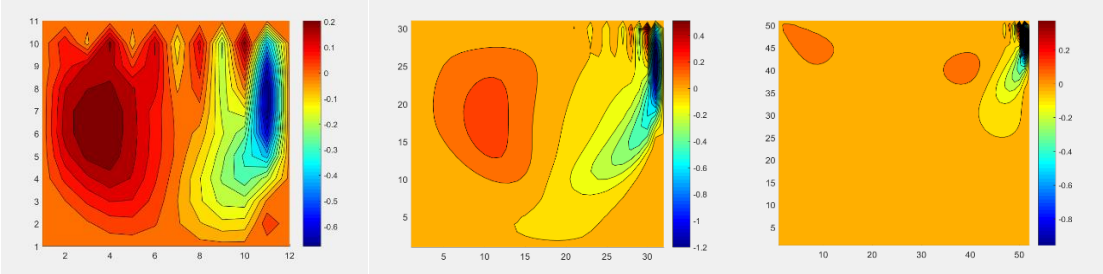

Figure 40: V (m/s), Mesh 10 x 10, 30 x 30, 50 x 50.

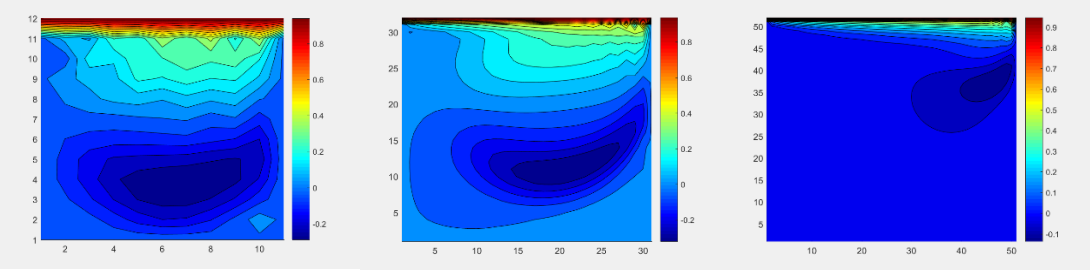

Figure 41: U (m/s), Mesh 10 x 10, 30 x 30, 50 x 50.

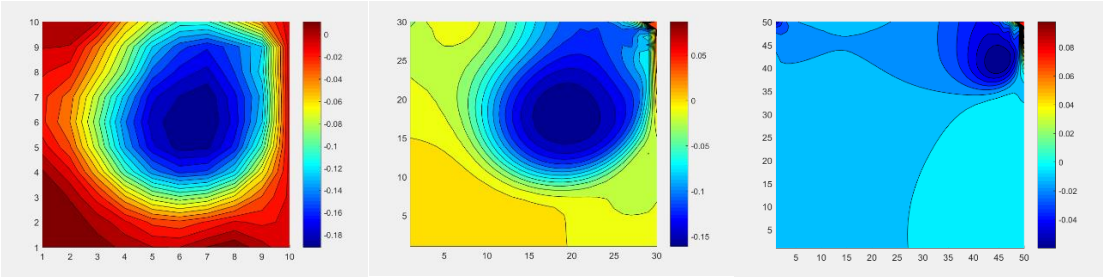

Figure 42: Pressure, Mesh 10 x 10, 30 x 30, 50 x 50

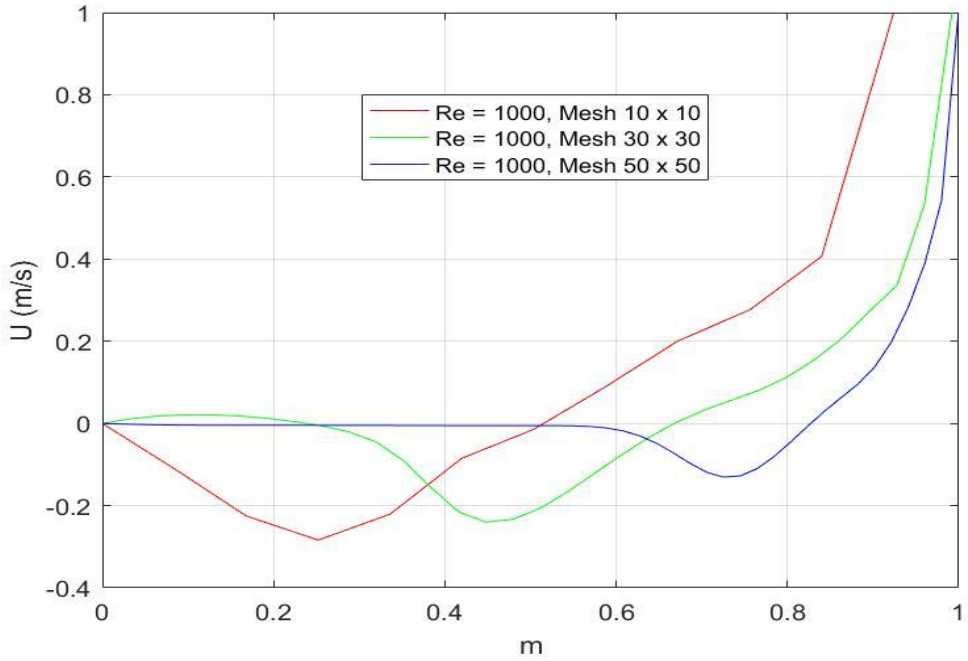

Figure 43: Mesh Comparison U(m/s) with Re = 1000.

Re = 2000

To conclude the results obtained from the simulation with a Re = 2000 are shown below, with a 10 x 10, 30x30, 50 x 50 mesh and a speed error less than 1e-6

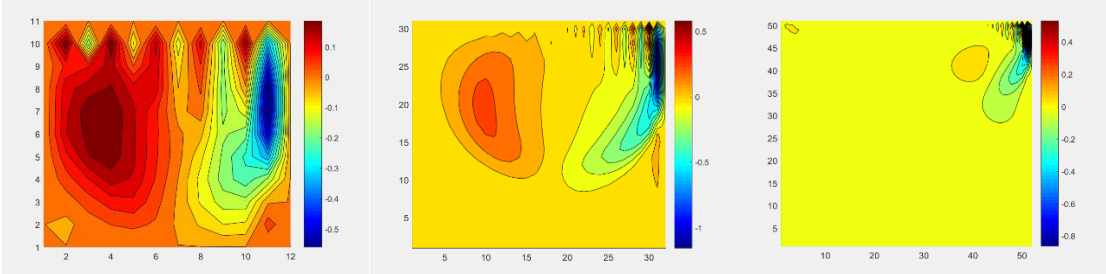

Figure 44: V (m/s), Mesh 10 x 10, 30 x 30, 50 x 50.

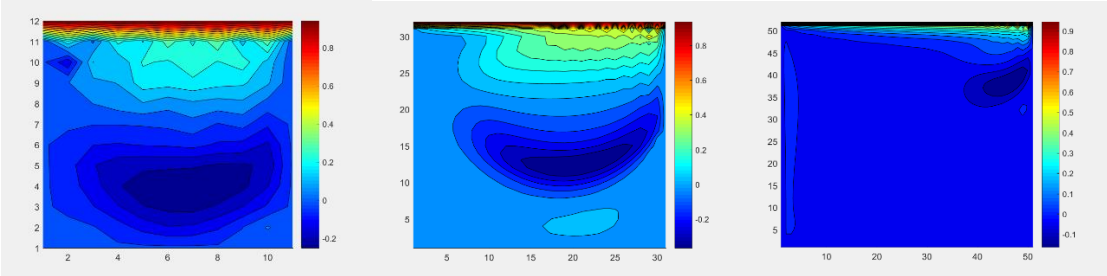

Figure 45: U (m/s), Mesh 10 x 10, 30 x 30, 50 x 50.

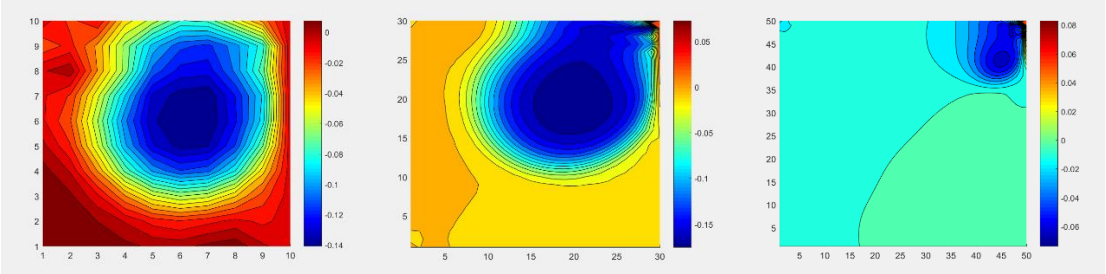

Figure 46: Pressure, Mesh 10 x 10, 30 x 30, 50 x 50.

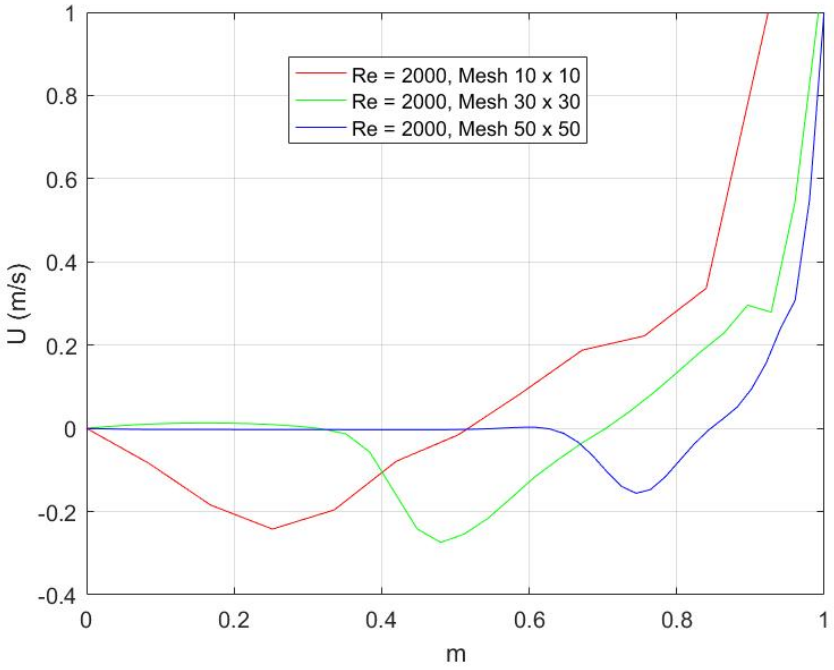

Figure 47: Mesh Comparison U(m/s) with Re= 2000.

10 x 10	20 x 20	30 x 30	40 x 40	50 x 50
3 min 1s	19min 55sec	38min 35sec	73min 6sec	97min 5sec

Table 10: Time comparison with different Mesh density.

To study the Driven cavity problem three different Mesh density were used (10 x 10, 30 x 30, 50 x 50), however, the table below shows a comparison of the number of steps and the computational time required for a 40 x 40 Mesh with different converge criteria.

Error_$\vec{v}$	n^0 steps	time
$\mathbf{5 \cdot 10^{-6}}$	150526	1h 13min
$\mathbf{1 \cdot 10^{-6}}$	581512	6h 9min

Table 11: Comparative table of the number of steps and the computational time required with a 40-cell grid for the different convergence criteria.

Re = 100 / 1000 / 2000

On the other hand, considering the physics behind the Reynolds number, the different results in the sections of Re = 100, Re = 1000 and Re = 2000 will be discussed below.

The section of Re = 100 is the case with the Reynolds number lower and therefore the more viscous fluid of the three. As we could intuitively foresee, it is the case that it presents lower speeds, since the viscous friction forces are higher, and the fluid is more difficult to move.

In the case of Re = 1000 the speeds are higher than in the previous case and the velocity profiles fit well to the results obtained.

However, in the case of Re = 2000, although the speeds are also higher, the comparison with the velocity profiles are quite different. The main reason may be that with that number of Reynolds we are at the limit between the laminar regime and the transition zone to the turbulent regime, so the numerical methods of resolution implemented are no longer the appropriate ones. These discrepancies in case of Re = 2000 we do not consider them an error of the program, on the contrary, this should happen since our code is not adapted to solve flows in the transition zone.

In cases with numbers of Reynolds 1000 and 2000, as we see in the figures, numerical instabilities appear in one of the corners, a logical fact since it is a simple code in which efficiency was not a priority. Until now, these instabilities have not been appreciated, probably because the time step we can afford to meet the Courant criterion in the case of Re = 100 is greater than in the cases of Re = 1000 and Re = 2000, therefore the number of the iterations necessary to reach the steady state are lower and the accumulation of errors is less. That is why we tried to reduce the time step for the two following simulations, although the same instabilities were obtained.

5.7 Summary Chapter

During this chapter we have studied the FSM, we have seen how to decouple the speed and pressure to obtain an intermediate speed and then the correct speed.

Regarding the temporal discretization, explicit schemes have been used, CDS (Central Difference Scheme) For the descretization of the temporal derivative, another explicit scheme of second order known as Adams-Bashforth for the terms $R(\vec{v})$ and finally a scheme of first backward order of Eulero for the pressure gradient.

We have seen the steps to follow for the resolution of the FSM, which are as follows;

- Calculate $R(\vec{v})$ using the initial velocity field
- Determine the intermediate speed
- Solve the poissson equation and obtain the field of pressures
- Correct the intermediate speed with the pressure of the previous step and evaluate the current speed of the fluid instantly n + 1.

Following later in the chapter we find the spatial discretization that is a fundamental part of this work. As in the previous cases, it has been adapted by the finite volume method, which is based on the direct discretization of the conservation equations of mass, motion and energy. The main advantage of this method is that the spatial discretization is carried out directly in the physical space of the problem. Therefore, there are no problems with the transformation between coordinate systems, as in the finite difference method. Another advantage of the method is the great flexibility it offers when using it in both structured and unstructured meshes. Due to all this, this method is one of the most used in CFD simulations.

On the other hand, if we look at the situation of the nodes in the meshes, two types are distinguished: the centered meshes and the displaced meshes (staggered). The displaced meshes work with the pressure in the center of the volume and the components of the velocity move half a cell towards the face of the same. The use of a shifted arrangement has the advantage that many of the terms that require interpolation with the centered mesh can be calculated directly without interpolation.

The algorithm of resolution that has been implemented has 3 parts that are the following;

- Case Definition
- Pre-Processing
- Iterative body

The definition of the case is an essential part of the whole process. At this point, the chosen physical problem is transformed into a set of discretized equations and the appropriate boundary conditions are established. Likewise, we opted for a specific spatial and temporal discretization, and finally the criteria of convergence of the program are chosen

Once the choice of the case has been stipulated, on the one hand, the physical data and the numerical parameters related to it are introduced, and on the other hand, the necessary calculations are made before the iterative body.

The iterative body is the most important part of the algorithm. This part is repeated many times until the convergence criterion is reached.

In this chapter to verify the methodology of the FSM, the DRIVEN CAVITY case has been studied. The problem consists in a closed cavity of infinite length, with a fluid in its interior and one of the walls moving at a constant speed.

The results have been divided into 3 parts;

- Re = 100
- Re = 1000
- Re = 2000

We have remained in the laminar regime since during the transition from laminar to turbulent errors can be found in the results.

A simple code has been created with MATLAB that solves the incompressible Navier-Stokes equations for the laminar regime. It has been verified that the code responds qualitatively to the physics that is expected from the fluid. Inside the cavity with the sliding lid is observed the recirculation of the fluid, moved by the friction with the lid. What is more, the quantitative comparison with commercial programs is very reasonable, it is observed as in viscous fluids the speed of the flow is small and as we approach the turbulent regime, greater divergences are found caused by the numerical simplicity of our implementation. These results can be considered positive considering the enormous complexity of the modern computational techniques of fluid dynamics and therefore we will conclude by saying that the objectives set at the beginning of the problem have been successfully fulfilled.

6.Introduction to Turbulence field

6.1 Introduction

Most of the flows encountered in engineering become unstable above a certain Reynolds number. Below that critical Reynolds number, flows are laminar. These instabilities cause a chaotic and random state of motion in which the velocity, pressure and temperature change continuously with time. This regime is called turbulent flow.

Turbulent fluctuations always have a three-dimensional spatial character creating rotational flow structures which are called turbulent eddies. To compute the turbulence simulation a large memory capacity is required.

This enormous computational cost is unfeasible for most computers. It can only be computed on supercomputers and the calculations last thousands of hours. For that reason, scientists and engineers are doing researches to develop numerical methods to capture the turbulent effects with a lower computational cost. The numerical methods are listed below:

- Large eddy simulation (LES): this method focuses on the behavior of larger eddies as well as the mean flow. Thus, the Navier-Stokes equations are filtered to compute the larger eddies and rejects the smaller eddies. The computational cost is high, although it is lower than the DNS. For that reason, it is starting to tackle complex CFD problems.

- Direct numerical simulation (DNS): This method needs a fine grid to solve the Kolmogorov length scales and sufficiently small-time steps to be able to resolve the fastest fluctuations. The computational cost is enormous, so it is only used for high accuracy flows in high-tech industries.

One of the biggest challenges at present in the field of complex systems is the knowledge of the turbulence phenomenon. This document will deal with different concepts related to the measurement of the turbulence phenomenon such as DNS or LES, as well as the properties that the Navier-Stokes equations must fulfill when dealing with turbulence.

To understand the basic concepts about the Navier-Stokes equations in the non-linear dynamics of turbulence, a simplified model will be presented that combines many of the mentioned aspects: Burgers Equation. In this section we will solve the Burgers equation in Fourier space.

6.2 Problem definition

The Navier-Stokes equations for incompressible flow in dimensionless form are:

$$\nabla \cdot \vec{v} = 0 \tag{6.1}$$

$$\frac{\partial \vec{v}}{\partial t} + (\vec{v} \cdot \nabla)\vec{v} = \frac{1}{Re}\Delta u - \nabla p \tag{6.2}$$

The Dutch scientist J.M.Burgers simplified the Navier-Stokes equations. With this simplification the equations can be studied in a single spatial dimension[13]:

$$\frac{\partial u}{\partial t} + u\frac{\partial u}{\partial x} = \frac{1}{Re}\frac{\partial^2 u}{\partial x^2} + f \tag{6.3}$$

As noted, the Burgers equation is not linear, so it can be expected to describe a phenomenon similar to turbulence. It has been verified that the Burgers equation does not present the main properties of turbulence, such as the sensitivity with the initial conditions. Despite this, it is still the best option to enter the turbulence phenomenon.

6.3 Numerical formulation

6.3.1 Burger's equation in Fourier Space

In this study the Burgers equation is expressed in the Fourier space.

$$\frac{\partial \hat{u}_k}{\partial t} + \sum_{k=p+q} \hat{u}_p \hat{u}_q q_i = -\frac{k^2}{Re}\hat{u}_k + f_k \qquad k = 0,1,2,\dots N \tag{6.4}$$

(6.5)

$$f_k = \begin{cases} so\ that, \dfrac{\partial \hat{u}_k}{\partial t} = 0 & for\ k = 1 \\ 0\ , & for\ k > 1 \end{cases}$$

Where the Fourier coefficient k of $u\ (x,\ t)$ corresponds to:

$$u(x) = \sum_{k\ =\ -\infty}^{k\ =\ +\infty} \hat{u}_k e^{ikx} \tag{6.6}$$

Transient term

$$\frac{\partial u}{\partial t} = \frac{\partial}{\partial t}\left(\sum_{k\ =\ -\infty}^{k\ =\ +\infty} \hat{u}_k e^{ikx}\right) = \sum_{k\ =\ -\infty}^{k\ =\ +\infty} \frac{\partial \hat{u}_k}{\partial t} e^{ikx} \tag{6.7}$$

Convective term

$$\begin{aligned} u\frac{\partial u}{\partial x} &= \left(\sum_{p\ =\ -\infty}^{p\ =\ +\infty} \hat{u}_p e^{ipx}\right) \frac{\partial}{\partial t}\left(\sum_{q\ =\ -\infty}^{q\ =\ +\infty} \hat{u}_q e^{iqx}\right) \\ &= \left(\sum_{p\ =\ -\infty}^{p\ =\ +\infty} \hat{u}_p e^{ipx}\right)\left(\sum_{q\ =\ -\infty}^{q\ =\ +\infty} iq\hat{u}_q e^{iqx}\right) \\ &= \sum_{p=\ -\infty}^{p=+\infty} \sum_{q=-\infty}^{q=+\infty} \hat{u}_p\ iq\hat{u}_q e^{i(q+p)x} \end{aligned} \tag{6.8}$$

Diffusive term

$$\frac{\partial^2 u}{\partial x^2} = \frac{\partial^2}{\partial x^2}\left(\sum_{k\ =\ -\infty}^{k\ =\ +\infty} \hat{u}_k e^{ikx}\right) = -\left(\sum_{k\ =\ -\infty}^{k\ =\ +\infty} k^2 \hat{u}_k e^{ikx}\right) \tag{6.9}$$

So, finally we obtained the following term for the equation (6.3) in Fourier space:

$$\sum_{k=-\infty}^{k=+\infty} \frac{\partial \hat{u}_k}{\partial t} e^{ikx} + \sum_{p=-\infty}^{p=+\infty} \sum_{q=-\infty}^{q=+\infty} \hat{u}_p \, iq\hat{u}_q e^{i(q+p)x} = \frac{1}{Re} \sum_{k=-\infty}^{k=+\infty} k^2 \hat{u}_k e^{ikx} + \sum_{k=-\infty}^{k=+\infty} f_k e^{ikx} \tag{6.10}$$

Which can be solved for each mode k

$$\frac{\partial \hat{u}_k}{\partial t} + \sum_{p+q=k} \hat{u}_p iq\hat{u}_q = \frac{1}{Re} k^2 \hat{u}_k + f_k \tag{6.11}$$

In addition, the following condition must be fulfilled:

$$\hat{u}_k = \overline{\hat{u}_{-k}} \tag{6.12}$$

This greatly facilitates the calculation since only the modes must be found corresponding to k = 0, 1, 2, ..., N, since the negative modes are given directly by the previous equation. The results of this problem will be exposed through the kinetic energy that is defined as:

$$E_k = \hat{u}_k \cdot \overline{\hat{u}_{-k}} \tag{6.13}$$

The energy $E_k \in \mathbb{R}$ of the K-th mode is obtained by taking the product of $\hat{u}_k$ with its complex conjugate.

6.3.2 Time Step

The following condition must be imposed so that the solution converges using an implicit scheme.

$$\Delta t < C \frac{Re}{N^2} \tag{6.14}$$

The parameter C has a value between 0 <C <1. Therefore, Δt must choose small enough for the system to converge on a stationary solution.

6.3.3 Spatial approximation

The discretization is based on the truncation of this series up to a finite amount of terms. This is:

$$u(x) = \sum_{k=-\infty}^{k=+\infty} \hat{u}_k e^{ikx} \approx \sum_{k=-N}^{k=+N} \hat{u}_k e^{ikx} \tag{6.15}$$

This reduces the infinite set of equations that would result of an infinite series to a set of equations. This number may be even reduced again considering assumption $\hat{u}_0 = 0$ and the fact that the solution to this problem has conjugate symmetry:

$$\hat{u}_k = \overline{\hat{u}_{-k}} \tag{6.16}$$

In the contribution of the convective term a special attention must be taken

$$\sum_{p+q=k} \hat{u}_p iq \hat{u}_q \tag{6.17}$$

So, given a mode K, the pair which contribute to the convective term are those which satisfy

$$p + q = k \tag{6.18}$$

With the spatial discretization the series is truncated to a range from -N to N. When computing the different combinations of modes and that accomplish (6.18), one should exclude those values which are out of bounds. This is

$$|p + q = k| < N \tag{6.19}$$

$$|p| < N\,;\ |q| < N \tag{6.20}$$

All the necessary interactions between modes (shaded region) are illustrated in the following representation. As it shown only the positive modes will be solved.

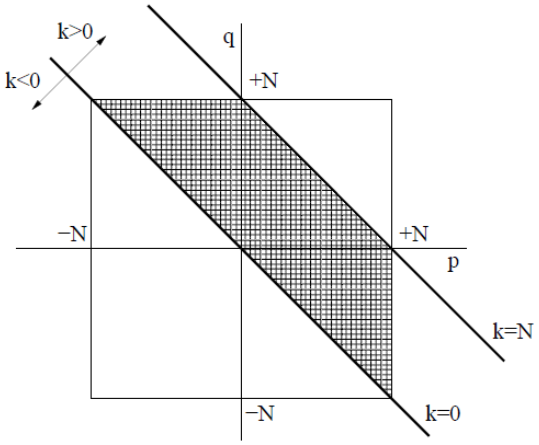

Figure 48: Positive interection between modes.

6.4 LES

Implementing a large eddy simulation (LES) model, which should improve the results of the coarser meshes. It consists basically in the addition of a non-dimensional viscosity that multiplies the diffusive term, which is determined by assuming some properties of the energy spectrum. This additional viscosity (turbulent) is calculated as follows:

$$v_t = v_t^{+\infty} \left(\frac{E_{k_N}}{k_N}\right)^{1/2} v_t^* \tag{6.21}$$

$$v_t^{+\infty} = 0.31\,\frac{5 - m}{m + 1}\,\sqrt{3 - m}\,C_k^{-3/2} \tag{6.22}$$

$$v_t^* = 1 + 34.5\,e^{-3.03\left(\frac{k_N}{k}\right)} \tag{6.23}$$

Where m is the slope of the energy spectrum, E_{k_N} is the energy at the cut-off frequency (k_N) and C_k is the Kolmogorov constant. In the case of the Burger's equation m ≈ 2 and C_k ≈ 0.4223. So, the equation for each mode that has to be solved using a LES model is:

$$\frac{\partial \hat{u}_k}{\partial t} + \sum_{p+q=k} \hat{u}_p iq \hat{u}_q = \frac{1}{Re} + v_{t_k} k^2 \hat{u}_k + F_k \tag{6.24}$$

6.5 Results

To compare the two methods (DNS and LES) different cases are solved.

Method	N	Re
DNS	20	40
DNS	100	40

Table 12: DNS Method with N modes and Re = 40.

Method	N	Re	C_k
LES	20	40	0.05
LES	20	40	0.4223

Table 13: LES Method with 20 modes and Re= 40.

The following figure shows the results provided by the created program. The results are compared with the reference provided by the CTTC.

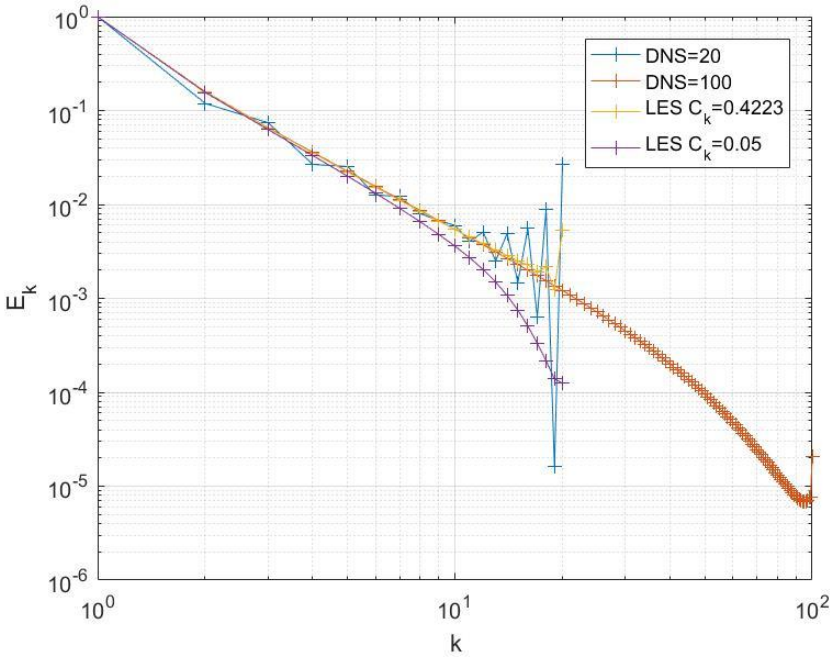

Figure 49: Results obtained with the simulation of the Burguers equation for Re = 40

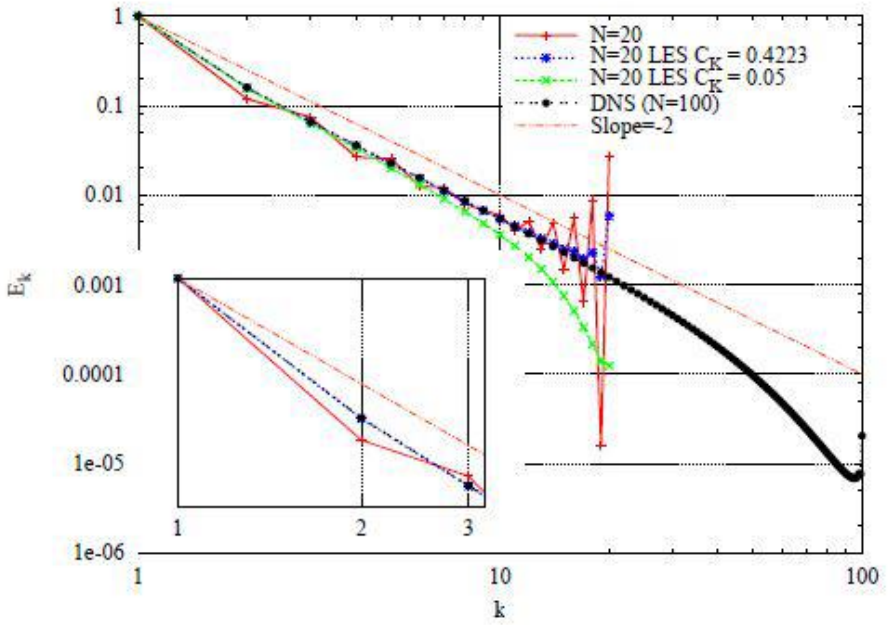

Figure 50: Reference solution for the energy spectrum of the steady-state solution of the Burgers equation with Re = 40 [14].

As seen in the graph, the results coincide with the reference. Now the results obtained in the simulations will be commented. Of both cases solved, it should be noted that although both implementations are solved quickly, the one related to the LES model decreases computer time to some extent and provides more precise results.

DNS

A large amount of modes needs to be simulated to have good results. with few modes the energy is not well distributed, the energy backscattering produces instabilities in all the scales, giving bad results even in the easiest zone to be solved.

LES

Kolmogorov 0.4523, the results obtained for the large scales are quite like the results obtained with the DNS of 100 modes and only some instabilities appear on the last modes.

Kolmogorov 0.05, the energy spectrum decays quicker than in the other simulations, there is a higher dissipation when increasing the modes.

6.6 Summary chapter

During this chapter we have studied the problem of turbulence with the Burger's equations. As noted, the Burgers equation is not linear, so it can be expected to describe a phenomenon similar to turbulence. It has been verified that the Burgers equation does not present the main properties of turbulence, such as the sensitivity with the initial conditions. Despite this, it is still the best option to enter the turbulence phenomenon.

We have discretized the equations in the Fourier space, in which we obtain three terms;

- Transient term
- Convective term
- Diffusive term

To subsequently reach a general formula with which we have raised the problem. We have seen the part that concerns the Time Step and the spatial approach that are a fundamental part when developing this case study.

For this case study two numerical methods have been developed;

- Large eddy simulation (LES): this method focuses on the behavior of larger eddies as well as the mean flow. Thus, the Navier-Stokes equations are filtered to compute the larger eddies and rejects the smaller eddies. The computational cost is high, although it is lower than the DNS. For that reason, it is starting to tackle complex CFD problems.

- Direct numerical simulation (DNS): This method needs a fine grid to solve the Kolmogorov length scales and sufficiently small-time steps to be able to resolve the fastest fluctuations. The computational cost is enormous, so it is only used for high accuracy flows in high-tech industries.

The results obtained as can be seen have similarity with the results provided by the CTTC. Given that the results are close to the theoretical ones, we can say that the problem posed at the beginning of this chapter has been successfully developed.

7.Conclusions

During the development of this work we have seen the resolution of the Navier Stokes equations in their incompressible form. We have started with a brief introduction of the positive aspects and the limitations that we find during the development of this project. Undoubtedly the use of codes for simulations in the field of computational fluid dynamics has helped to improve and efficiency in the aerospace industry and everything related to it.

The mathematical formulations that we have found throughout the second chapter have helped us to understand and subsequently solve the cases that we will find later in the fourth and fifth chapter. In this work, simple structured meshes have been implemented since the case studies are not so complex. We have varied only the density of the meshes with the aim of obtaining more accurate results to the references, which has been proven that denser the mesh, the better results we get, but the negative aspect in all this is the computational time that is much highest.

Another parameter that we have changed during the simulations the convergence criterion, we have used simple criteria that adapt to the physics of the problem. For the MatLab program we have decided that the simulation ends when the relative difference of the speed between two consecutive time steps is less than a certain value. On the other hand, we have implemented two types of Solvers, Point by Point and Line by Line. The precision in the results obtained by both solvers is almost identical therefore in this work we have used the Line by Line for the case of Convection Heat Transfer and the Point by Point for the other cases.

For all cases of studies, codes have been created that solve the incompressible Navier-Stokes equations for the laminar regime. The programs have been validated by comparing the results obtained with the References provided by the CTTC and with which the efficiency of the programs has been verified.

To conclude it can be said that the objectives set at the beginning of the development of this project have been achieved, the phenomenologies presented by the study of the Navier-Stokes equations have been observed, the Navier-Stokes equations have been applied to simple cases of computational fluid dynamics with the aim of introducing us in this field. Throughout the development and analysis of the different cases, false diffusion phenomena can be observed which can produce an inadequate mesh or a Reynolds number that is too high or due to convergence problems.

7.1 Future Work

As far as future work is concerned, it would be possible to improve the codes made in this project, giving a greater precision to the results and thus be able to get closer to the theoretical data.

For the development of this work MATLAB has been used as a programming language, we have used simple functions without complex structures. For the following works we could make use of another programming language like C ++ in which it would help us in a quick resolution of the cases and since C ++ is a better-known programming language it would help us to confront us with other working groups and make a more precise code with better results.

The time available is a key factor when performing a job like this, therefore, to get better results many simulations have to be done to compare all the results obtained and decide which is closer to the physical problem.

The mesh is another key point for this type of work, in the future it could be implemented unstructured meshes to obtain a greater precision in the results. For this first one must make a study of the problem and then think that the mesh is appropriate for that case. Working with unstructured meshes helps analyze cases where the geometry of the problem is more complex.

During this work we have analyzed simple cases, the most convenient thing in the future is to analyze more complex cases and enter more in what concerns the field of turbulence since without doubt during the study of computational fluid dynamics cases we find these problems.

Key points for future works;

- Language programming
- Work with different types of Mesh
- Analyze Turbolent cases
- More time for simluations

8.Task Planning

In the table below, you can see a description of the tasks that must be done during the work, as well as the relationship between them and their approximate duration. In addition to this table, the Gantt chart is attached where you can see graphically the duration and dependence of these tasks.

Task	Description	Precedence	Time[h]
A	Estudios de las ecuaciones de Navier-Stokes en su forma incompresible e Introduccion al campo de las turbolencias.	-	100
B	MATLAB ampliación de los conocimientos.	A	35
C	Estudio técnicas de Mallado (Finite Volume Method).	B	20
D	Desarrollo códigos para los diferentes casos de estudio de las ecuaciones de conveccion-difusion y análisis de estos.	A, B, C	100
E	Estudio y Desarrollo algoritmos FSM (Fractional Step Method).	A, B, C	75
F	Verificacion analisis de los resultados FSM.	F	35
G	Desarrollo de los algoritmos y análisis de los resultados Burger's equation para los casos DNS Y LES.	A, B, C, F	25
H	Redacción del reporte correspondiente a los casos estudiados.	A	75

Table 14: Task Planning with description of each task and time.

Task	1	2	3	4	5	6	7	8	9	10	11	12	13	14	15	16
A																
B																
C																
D																
E																
F																
G																
H																

Table 15: Gantt chart

9.Enviromental Impact

For the accomplishment of this work two important things have been used, paper in what concerns the calculations and studies of this subject and the electrical energy for the development of the codes and the simulations.

The environmental impact could be measured in how many hours electric power is used to make the simulations, but we must know that using this method of fluid dynamics simulations no longer have to create models at scales which would lead to a greater environmental impact by the use of larger materials which once done the tests would have to be thrown away since sometimes destructive tests are made.

On the other hand, the use of paper is true that doing calculations by hand requires the use of paper, but we can lower the environmental impact using recycled paper and in turn recycling used paper.

In conclusion, two main Environmental impact factors are considered for the realization of this project;

- Paper consumption
- Electric consumption

For the development of this work we have tried to minimize the environmental impact by following what has been said in the paragraphs above, for which the environmental impact of this work has been minimal.

Bibliography

[1] "Conservation Equations Applied Computational Fluid Dynamics," 2006.

[2] R. S. Subramanian, "Reynolds Number," pp. 1–3, 1883.

[3] "Patankar 1980.pdf." .

[4] J. H. Ferziger and M. Peric, *Computational Methods for Fluid Dynamics*. 2002.

[5] Encyclopædia Britannica, "Navier-Stokes Equation," *Encycl. Br. Ultim. Ref. Suite.*, 2015.

[6] C. F. Dynamics, "A1- NUMERICAL SOLUTION OF CONVECTION -," vol. M, pp. 1–15.

[7] M. S. Darwish, "A new high–resolution scheme based on the normalized variable formulation," *Numer. Heat Transf. Part B Fundam.*, vol. 24, no. 3, pp. 353–371, 1993.

[8] H. K. Versteeg and W. Malalasekera, "An Introduction to Computational Fluid Dynamics - The Finite Volume Method," *Fluid flow handbook. McGraw-Hill …*. p. 267, 1995.

[9] CTTC - Universitat Politècnica de Catalunya, "A Two-dimensional Transient Conduction Problem," pp. 3–5, 2014.

[10] "Verification strategies for the convection-diffusion equation," pp. 1–5.

[11] "Introduction to the Fractional Step Method. CTTC, Centre Tecnològic de Transferència de Calor. Terrassa, Spain : Universitat Politecnica de Catalunya, 2013."

[12] "CTTC - Universitat Politècnica de Catalunya, 'Fractional Step Method Staggered Meshes,' 2014." .

[13] "Computational engineering Theory UPC slides."

[14] T. Navier-stokes, "Burgers equation in Fourier space," vol. 4, no. 4, pp. 1–8, 2014.